

THE UNIVERSITY OF MICHIGAN
OFFICE OF RESEARCH ADMINISTRATION
ANN ARBOR

SIMRAR: SIMULATED RECEIVER AND RECORDER FOR
STATISTICAL MEASUREMENTS


Technical Report No. 118

2899-43-T

Cooley Electronics Laboratory
Department of Electrical Engineering

By: ^{mmis} D. W. Fife

Approved by:


A. B. Macnee

Project 2899

TASK ORDER NO. EDG-3
CONTRACT NO. DA-36-039 sc-78283
SIGNAL CORPS, DEPARTMENT OF THE ARMY
DEPARTMENT OF ARMY PROJECT NO. 3A99-06-001-01

January 1961

THE UNIVERSITY OF MICHIGAN
ENGINEERING LIBRARY

Ergo

UMR

1459

PREFACE

The simulation equipment described in this report has evolved over a period of six years with the primary objective of supporting signal detection studies. Many signal detection problems are characterized by the fact that it is much easier to specify what the optimum receiver is than to calculate the performance of this optimum receiver. The original work of T. G. Birdsall and W. W. Peterson in the area (Ref. 1) pointed this problem up very clearly, and as a result W. W. Peterson conceived and designed the original SIMRAR system in 1954. Over the years since that time many workers have contributed to the improvement, modification, and development of this equipment to its present form. Particular credit is due to Mr. R. R. McPherson who, more than any other one individual, was responsible for bringing the original concept to a useful fruition. More recently Mr. Quintus C. Wilson, II and Mr. D. W. Fife have contributed extensively to further modification and improvements of the equipment.

As it exists today, SIMRAR is useful for a much wider class of problems than was considered when it was first planned. It has found application in our group in a study of tracking errors in a fire control radar, in studies of the properties of pseudo-random waveforms, and in the study of panoramic receiver detection problems.

Because of the long period of evolution of this equipment, there are portions of the circuit which are not the best designs possible. If we were to design a new unit today, there are certainly several circuits which would be modified. Other workers in this area who are considering the duplication of this equipment or the development of similar equipment are invited to write or visit the Cooley Electronics Laboratory to discuss their plans.

TABLE OF CONTENTS

	Page
PREFACE	iii
LIST OF ILLUSTRATIONS	vi
ABSTRACT	x
CHAPTER 1. INTRODUCTION	1
CHAPTER 2. GENERAL DESCRIPTION OF EQUIPMENT	3
2.1 Counter Chassis	3
2.2 Control Chassis	3
2.3 Main Simulator Chassis	4
2.4 Preset Counter	4
2.5 Miscellaneous	5
CHAPTER 3. FUNDAMENTAL DESCRIPTION OF OPERATION	5
3.1 Fixed Time Duration Tests	5
3.2 Sequential Tests	9
3.3 Data Collection	12
CHAPTER 4. COMPONENT CIRCUITS OF SIMRAR	14
4.1 Counter Chassis	14
4.2 Control Chassis	18
4.2.1 General Description	18
4.2.2 Timing Control	20
4.2.3 Cycling Control Circuit	24
4.2.4 2 kc Perturbation Oscillator	32
4.3 Main Simulator Chassis	35
4.3.1 Tuned Amplifier and Detector	35
4.3.2 Operational Amplifiers and Function Generator	40
4.3.2.1 Circuit Description	40
4.3.2.2 Setup Procedure for Function Generator	42
4.3.3 Voltage Divider	47
4.4 Preset Counter	47
4.5 Power Supply	53
4.6 Miscellaneous Equipment	57
4.6.2 Delayed Pulse Generator	57
4.6.3 Squaring Circuit	61
CHAPTER 5. DETAILED DESCRIPTION OF A TYPICAL SIMULATION	63
CHAPTER 6. PERFORMANCE OF SIMRAR IN STATISTICAL MEASUREMENTS	69
CHAPTER 7. SUMMARY	78
REFERENCES	79
DISTRIBUTION LIST	80

LIST OF ILLUSTRATIONS

Figure		Page
1	Front (a) and back (b) views of SIMRAR.	3
2	Simulation of general fixed time duration detection problem.	7
3	Simulation of sequential test.	9
4	Comparison of output waveforms on (a) fixed time (b) sequential tests.	11
5	Standard deviation of measured probability.	13
6	Amplitude discriminator.	15
7	Gain-frequency response of discriminator amplifier.	17
8	Front view of counter chassis.	18
9	Rear view of counter chassis.	19
10	Front view of control chassis.	19
11	Top view of control chassis.	20
12	Control chassis plugboard connections.	20
13	SIMRAR timing control.	23
14	Control circuit.	25
15	Cycling control circuit relay sequence.	26
16	Timing waveform (A8). 20 v/cm vertical 50 ms/div horizontal.	27
17	#11 2D21 grid waveform. 20 v/cm vertical 50 ms/cm horizontal.	27
18	6AQ5 grid waveform (C3) 20 v/cm vertical 50 ms/cm horizontal.	27
19	6AQ5 plate waveform (All) 60 v/cm vertical 50 mc/cm horizontal.	27
20	IM2 relay voltage waveform. 60 v/cm vertical 50 ms/cm horizontal.	28
21	AP17D pulse waveform. 60 v/cm vertical 50 ms/cm horizontal.	28

LIST OF ILLUSTRATIONS--Continued

Figure		Page
22	Termination supply waveform. 60 v/cm vertical 50 ms/cm horizontal.	28
23	Push-to-stop switch contact waveform (A3). 60 v/cm vertical 50 ms/cm horizontal.	28
24	+125 volts, SN-alternative post-interval decision time (A2). 60 v/cm vertical 50 ms/cm horizontal.	29
25	+125 volts, SN-alternative, continuous decision time (A2). 60 v/cm vertical 50 ms/cm horizontal.	29
26	+125 volts, N-alternative, post-interval decision time (B2). 60 v/cm vertical 50 ms/cm horizontal.	29
27	+125 volts, N-alternative, continuous decision time (B2). 60 v/cm vertical 50 ms/cm horizontal.	29
28	2 kc oscillator schematic.	32
29	2 kc oscillator output waveform. 20 v/cm vertical .165 ms/cm horizontal.	32
30	Operational amplifier 3 schematic.	33
31	Gain-frequency response of amplifier 3.	34
32	Main simulator chassis, front view.	35
33	Tuned amplifier-detector, back view.	36
34	Tuned amplifier and envelope detector.	37
35	SIMRAR 1 kc/s tuned amplifier; gain vs. frequency.	38
36	SIMRAR 10 kc/s tuned amplifier; gain vs. frequency.	38
37	Gain-frequency response of envelope detector filter.	39
38	Function generator, back view.	40
39	Amplifier #2 and function generator.	41
40	An approximation to a function for simulation.	43
41	Function generator setup diagram.	45
42	Function generator setup, front view.	46
43	Voltage divider schematic.	50

LIST OF ILLUSTRATIONS--Continued

Figure		Page
44	Preset counter schematic.	48
45	Preset counter, front view.	51
46	Preset counter, back view.	51
47	Power supply schematic diagram.	54
48	Power supply, front view.	55
49	Power supply, rear view.	55
50	Power supply plug connections.	57
51	Delayed pulse generator schematic.	57
52	10 kc/s pulse output of delayed pulse generator. 20 v/cm vertical 10 ms/cm horizontal.	60
53	Delayed pulse generator--pulse delay test point waveform 60 v/cm vertical 10 ms/cm horizontal.	60
54	Delayed pulse generator-pulse gate test point wave.	61
55	Delayed pulse generator, back view.	61
56	Schematic diagram of squaring circuit.	62
57	Simulation for broadband reception of constant amplitude signal completely known except for phase.	64
58	SIMRAR noise calibration curve.	66
59	Receiver operating curve of broadband receiver.	67
60	Tuned amplifier output, signal and noise present.	67
61	1 kc/s tuned amplifier output: noise alone present. 20 v/cm vertical 5.9 ms/cm horizontal.	68
62	Detector output: signal and noise present. 20 v/cm vertical 5.9 ms/cm horizontal.	68
63	Detector output: noise alone present. 20 v/cm vertical 5.9 ms/cm horizontal.	68
64	Integrator output; SN and N waveforms on two consecutive trials. 20 v/cm vertical 5.9 ms/cm horizontal.	68

LIST OF ILLUSTRATIONS--Continued

Figure		Page
65	SIMRAR amplifier dc drift after 25-minute warmup.	70
66	Resolution of threshold level in amplitude discriminators.	76

ABSTRACT

The design and operation of SIMRAR, a simulated receiver and statistical recorder, are described. The equipment is used for statistical studies of signal detection by receivers, and for general statistical measurements.

SIMRAR: SIMULATED RECEIVER AND RECORDER
FOR STATISTICAL MEASUREMENTS

1. INTRODUCTION

SIMRAR (SIMulated Receiver And Recorder) is a special purpose analog simulator, incorporating circuits for statistical measurements and recording. The equipment was designed and built at this laboratory, and has been used in experimental studies of several receiving systems for the detection of signals in noise.

SIMRAR is composed, in part, of the basic elements of a receiver: a bandpass (IF) filter-amplifier and linear envelope detector. In addition, several operational amplifiers and a function generator provide versatility in simulation of additional (video) filtering and an arbitrary detector law. The input to the bandpass filter, which corresponds to the output of the mixer in a physical receiver, is usually obtained from a simulation of the received signal and the noise by other components included in SIMRAR. This permits a flexibility in the simulation of input signals so that a wide variety of receivers can be studied.

The problem of detecting the presence of a signal in noise may be looked upon as a statistical decision process having four possible outcomes, as follows:

- hit: a correct decision that a signal is present;
- miss: a decision that no signal is present (noise alone) when a signal is present;
- false alarm: a decision that a signal is present when only noise is actually present;
- quiet: a correct decision that no signal is present.

A hit and a quiet correspond to correct decisions, while a miss and a false alarm are errors. Since a miss and a quiet are the events complementary to a hit and a false alarm, respectively, the signal detection performance can be measured on a statistical basis by the relative number of hits and false alarms over a large number of detection trials. That is, the signal detection performance of a receiver can be evaluated in terms of the hit (correct detection) probability when signal and noise are present at the input, and the false alarm probability when noise alone is present.

Reference 1 discusses the general problem of signal detection, including the criterion to be used in making the decision, and the optimum receiver design for a variety of signals. In this approach, the receiver input generates a decision function as the receiver output, and the decision "signal present" is made whenever the amplitude of this output exceeds a threshold level. Accordingly, SIMRAR includes amplitude discriminating circuits with variable threshold levels.

To obtain estimates of the detection and false alarm probabilities, counters are provided to record the number of "signal present" decisions on each of two alternative inputs, signal and noise, and noise alone. Timing and control circuits are used to accomplish continuous cycling until a large number of detection trials on each alternative have been obtained. The probability estimates are then the ratios of the number of "signal present" decisions and the number of detection trials on each alternative input. The availability of trigger pulses and relay gates from the control circuits permits slaving external equipment to SIMRAR.

2. GENERAL DESCRIPTION OF EQUIPMENT

2.1 Counter Chassis

Figures 1(a) and 1(b) are front and back views of SIMRAR, showing the counter chassis and other major parts of the equipment.

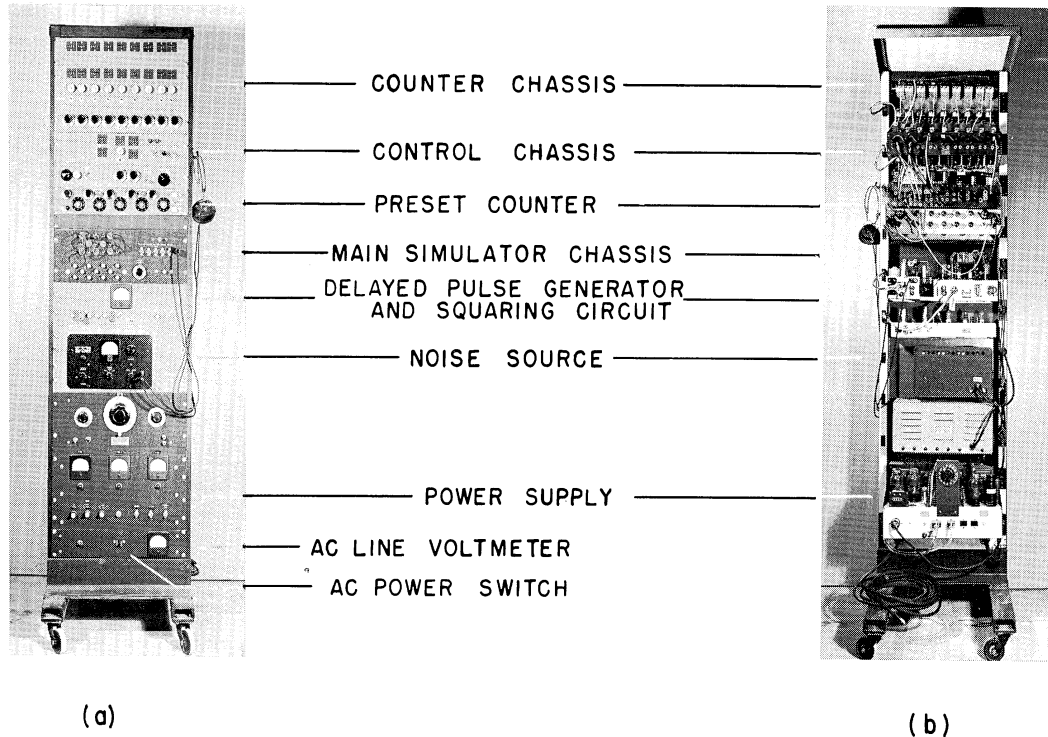


Fig. 1. Front (a) and back (b) views of SIMRAR.

The counter chassis contains 9 amplitude discriminator circuits, 2 counters for each discriminator (one for each alternative input to the receiver simulation), and a 10-turn potentiometer for setting the threshold level of each discriminator. The main part of each discriminator is a bandpass amplifier centered at 2 kc, with a gain of +54.5 db and a 3 db bandwidth of 4.24 kc. The discriminators respond to low frequency inputs from 0 to +60 volts. The counters can record up to 9,999 counts.

2.2 Control Chassis

The control chassis houses the timing control circuit which

determines the time duration of each detection trial, and the cycling control circuit which provides for automatic cycling to accomplish a large number of trials. The minimum useful time duration per trial is 30 milliseconds. (On post-interval decisions, an effective sampling time of 9 milliseconds is available.) The maximum available duration is 3.5 seconds, but an external timing source may readily be used to extend this range. Also included on the control chassis are an additional amplitude discriminator (No. 10) and its counters, a total trials counter, counters to record total trials per alternative, a 2-kc oscillator, and the No. 3 operational amplifier. This amplifier has an open loop gain of +58 db, 3 db bandwidth of 1.75 kc, and dynamic range of ± 60 volts.

2.3 Main Simulator Chassis

The main simulator chassis contains most of the receiver simulation. It includes a bandpass amplifier with selectable center frequencies of 1 kc and 10 kc, and nominal total bandwidths of 22 cps and 400 cps, respectively. The corresponding gain at the center frequency is +67 db and +87 db, respectively. A linear envelope detector utilizes a diode and a low-pass Butterworth filter having a cutoff frequency of 400 cps. A voltage divider is included to provide fixed dc voltages continuously adjustable in several ranges up to 300 volts. There are also two operational amplifiers on this chassis, one of which is an integral part of the function generator. These amplifiers have an open loop gain of +58 db, and a 3-db bandwidth of 1.75 kc. The dynamic range of the amplifiers is ± 60 volts.

2.4 Preset Counter

The preset counter is used to stop the cycling of SIMRAR when

a preset number of total trials has been completed. Three input trigger modes are available. Operation of a relay in the circuit, and a voltage pulse output at completion of the selected number of trials make this equipment useful in other applications.

2.5 Miscellaneous

The noise source in SIMRAR is a General Radio Type 1390A. The output is adjustable to as much as 5 volts rms, in bandwidths of 20 kc, 500 kc or 5 Mc, as selected.

The power supply furnishes ac power for filaments, + and -300 volts for plate supply to the circuits, and +125 volts dc for recording in SIMRAR.

A delayed pulse generator circuit furnishes sine-wave pulses of variable duration for pulse signal experiments with the 10-kc tuned amplifier in the receiver simulation. A squaring circuit is also part of the SIMRAR equipment. Table I summarizes the characteristics of the more important components which have been described here.

3. FUNDAMENTAL DESCRIPTION OF OPERATION

3.1 Fixed Time Duration Tests

In this section the basic operation of SIMRAR and method of simulation is explained. The primary application of SIMRAR in the past has been in simulation of detection situations involving a fixed time duration for observation of the receiver input on each detection trial. Figure 2 is a block diagram of the simulation for a general detection problem of this kind.

The signal is supplied from an external simulation. For example, if the signal is to be a continuous, single-frequency signal of arbitrary phase, an audio oscillator is sufficient. Wideband, white

TABLE I

SUMMARY OF SIMRAR COMPONENT CHARACTERISTICS

UNIT	NUMBER	CENTER FREQ.	BANDWIDTH	GAIN	RANGE	
Positive Amplitude Discriminator	10	2 kc	4.24 kc	+54.5 db	0 to +60 v	Trips counter when low pass input exceeds threshold level, variable from 0 to +60 volts.
Negative Amplitude Discriminator	1	2 kc	4.24 kc	+54.5 db	0 to -60 v	Identical to positive discriminator but operates for negative inputs only.
Tuned Amplifier	2	1 kc 10 kc	22 cps 400 cps	+67 db +87 db	0 to ±60 v 0 to ±60 v	Mounted on same chassis. Characteristics determined by switch selection.
Linear Envelope Detector	1	-	low pass* 400 cps	-1.5 db	0 to ±60 v	Output polarity selected by switch.
Operational Amplifier	3**	-	low pass 1.75 kc	+58 db open loop	0 to ±60 v	Used with proper impedances in input and feedback paths to obtain arbitrary gain and filtering.
Function Generator	1	-	Determined by operational amplifier characteristic		0 to + 60 v output	Used in conjunction with operational amplifier to simulate increasing functions with positive slope.
Voltage Divider	1	dc only			0 to ±300 v	Provides fixed DC voltages tapped off power supply. Continuous adjustment in 5 ranges.
Noise Generator	1	-	20 kc 500 kc or 5 Mc	-	0 to 5 v rms	General Radio Type 1390 giving selectable bandwidths of white Gaussian noise.

* Applies to detector filter

** One amplifier is integral part of function generator

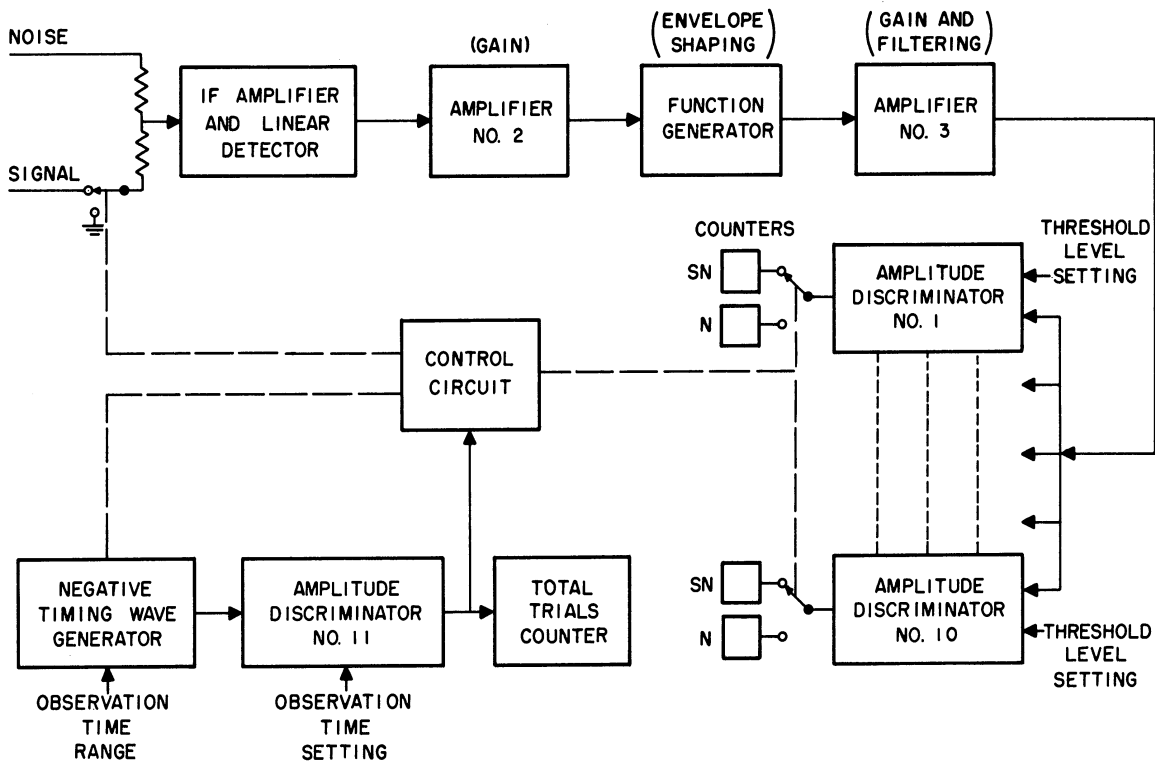


Fig. 2. Simulation of general fixed time duration detection problem.

Gaussian noise is supplied from the noise generator which is a part of SIMRAR. The resistive adding circuit at the IF input can be scaled to give the desired range of input signal-to-noise ratio for the available range of variation of signal amplitude and noise power. The center frequency of the IF filter can be selected as either 1 kc/s or 10 kc/s.

Operational amplifier No. 2 is usually used to obtain the proper gain before the function generator. Amplifier No. 3 can be used for additional gain and/or filtering, with suitable impedances in the input and feedback paths. Often, it is used as an integrator or video amplifier. Provision is made to restore the amplifier circuit to a zero initial condition at the end of each detection trial, if desired. The function generator can be used to generate a desired envelope shaping function (detector characteristic).

In the fixed time duration tests, the output of the simulated receiver is fed from amplifier No. 3 to the 10 amplitude discriminator circuits, for which the threshold levels have been preset according to the expected distribution of the amplitude. The control circuit of SIMRAR alternately switches the receiver input from signal-and-noise (SN) to noise alone (N), and also switches the output of the discriminator circuits to accomplish recording on the counters corresponding to the alternative input during the observation interval. Each amplitude discriminator may be looked upon as a decision device which trips a counter to indicate the decision "signal present" whenever the receiver output amplitude exceeds the threshold value (decision level) which has been set for it. In many detection situations it is best to delay the decision until the observation time is completed. The control circuit of SIMRAR provides for making the decision (recording) continuously during the observation interval or at the end of the observation interval (post interval decision).

When the observation interval is completed, SIMRAR requires a fixed dead time to complete recording and resetting before another observation or detection trial can be undertaken. The complex switching functions which accomplish this are incorporated in the control circuit and will be described fully in a later section. For the present, the primary functions of interest are switching the receiver input, switching the recording circuits to the proper counters, and resetting the timing wave generator. The timing wave in fixed time tests is a negative-going sawtooth, the slope of which is determined by the position of the observation time range switch. The length of the observation time interval is set by the threshold level of the No. 11

discriminator circuit. When the timing wave reaches this value, the discriminator circuit operates, advancing the total trials counter, and setting the switching operation of the control circuit in motion. In practice, the time duration of the observation interval is set using external equipment (usually an oscilloscope) to monitor the value obtained.

3.2 Sequential Tests

Another detection problem which may be simulated with SIMRAR is a sequential test, for which the receiver observes the input until sufficient information has been obtained to make a decision. In this case the observation time is not fixed, but depends on the time required for the receiver to make the decision achieving the desired detection performance. SIMRAR then measures the distribution of the decision times. Figure 3 illustrates the simulation for a general problem

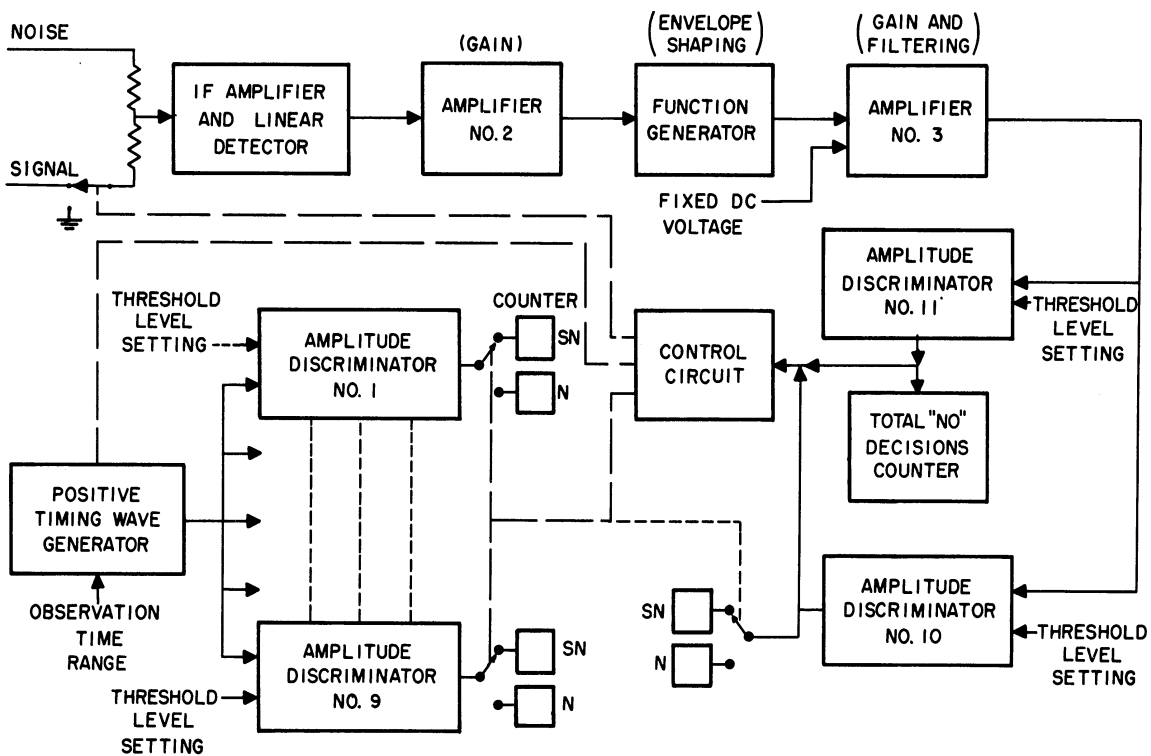


Fig. 3. Simulation of sequential test.

of this type.

As in fixed time duration tests, the IF amplifier, function generator, and operational amplifiers are set up to simulate the receiver, with suitable input signals and noise. Then amplitude discriminators No. 10 and No. 11 are used as decision mechanisms which terminate the observation when a decision is made. If only one discriminator were used in this manner, then every observation would terminate in a correct detection or a false alarm, depending upon whether signal-and-noise or noise alone was present during the observation. The signal detection performance achieved would therefore always be 100 percent correct detection at 100 percent false alarm.

In order to accomplish detection performance other than 100 percent correct detection and 100 percent false alarm, it is necessary to set up the decision device to either accept or reject the hypothesis under test on each alternative. Thus two discriminator circuits are required. In Fig. 3 the No. 11 discriminator performs the decision of rejecting the hypothesis on both alternatives. The No. 10 discriminator performs the acceptance decision (correct detection or false alarm) on the alternatives. Recording is made of the total rejections, the number of false alarms, and the number of correct detections. The total number of trials is the sum of these three, and the number of trials on each alternative is half of the total.

Since the No. 11 discriminator responds only for negative inputs, whereas the No. 10 responds only for positive inputs, it is required that the output of amplifier No. 3 have the possibility of being of either polarity at any instant of time. The output of the function generator

is always negative in the simulation of Fig. 4. Hence a positive fixed dc voltage is added at amplifier No. 3 to make its output be of either polarity. The threshold level of the No. 10 discriminator is adjusted until the desired detection performance (correct detections versus false alarms) is achieved.

The difference between a fixed time test and a sequential test may be clarified by Fig. 4. This illustrates a typical output

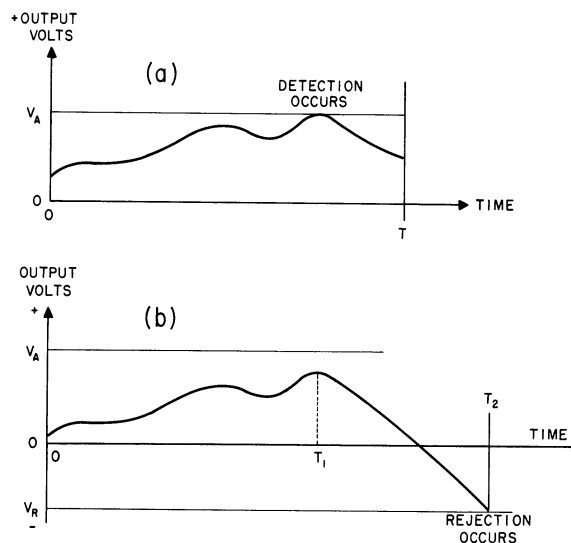


Fig. 4. Comparison of output waveforms on (a) fixed time (b) sequential tests.

waveform on one detection trial for the two tests with the same simulation in regard to signals and noise, IF amplifier, function generator and other gains and filtering. The output for the sequential test is lower by a constant amount due to the addition of the dc voltage at amplifier No. 3. Now, in the fixed time test an observation is always of time duration T . For the output illustrated in Fig. 4 a detection occurs, since the threshold level, V_A , is exceeded. On the sequential test, however, the observation of this output waveform lasts beyond T , extending to the time when a rejection decision occurs, T_2 . Note that if the upper threshold, V_A , had been lower, an acceptance decision could have occurred at T_1 , in which case the observation would have ended there. (Lowering the threshold would, of course, result in a higher probability of correct detection, and a higher probability of a false alarm.) In the fixed time test, a time interval is chosen and detection performance is

measured. In a sequential test, detection performance is selected and the distribution of decision time is measured.

3.3 Data Collection.

The recording circuits of SIMRAR may be used exclusive of the receiver simulation to obtain statistical measurements of the amplitude distribution of any voltage input. After a sufficient number of trials the counter readings yield good estimates of the probabilities, $P(\text{voltage input} \geq a)$, where a is the threshold level of the discriminator circuits. These estimates are obtained by dividing the counter reading by the number of trials taken. Since there are ten discriminator circuits, probability estimates can be obtained for ten different threshold values. In studies of signal detection problems, for which the receiver simulation has two alternative inputs, the counter pair of each discriminator circuit gives estimates of the probabilities, $P_{\text{SN}}(\text{receiver output} \geq a) = P_{\text{SN}}(A) = \text{detection probability}$, and $P_{\text{N}}(\text{receiver output} \geq a) = P_{\text{N}}(A) = \text{false alarm probability}$, for the threshold level, a , of the discriminator circuit. These estimates are found by dividing the counter reading by the number of trials taken on the alternative (half of the total number).

The reliability of the probability estimates obtained depends upon the number of trials taken and the true probability, the accuracy of the equipment notwithstanding. If n is the number of trials taken, and p is the true probability, the standard deviation of the measured probability is,

$$\sigma = \sqrt{\frac{p(1-p)}{n}} \quad (1)$$

Figure 5 is a plot of Eq. 1 against the true probability, p , for several values of n . As can be seen from this figure, the statistical inaccuracy of a measurement of 100 trials is rather large. The

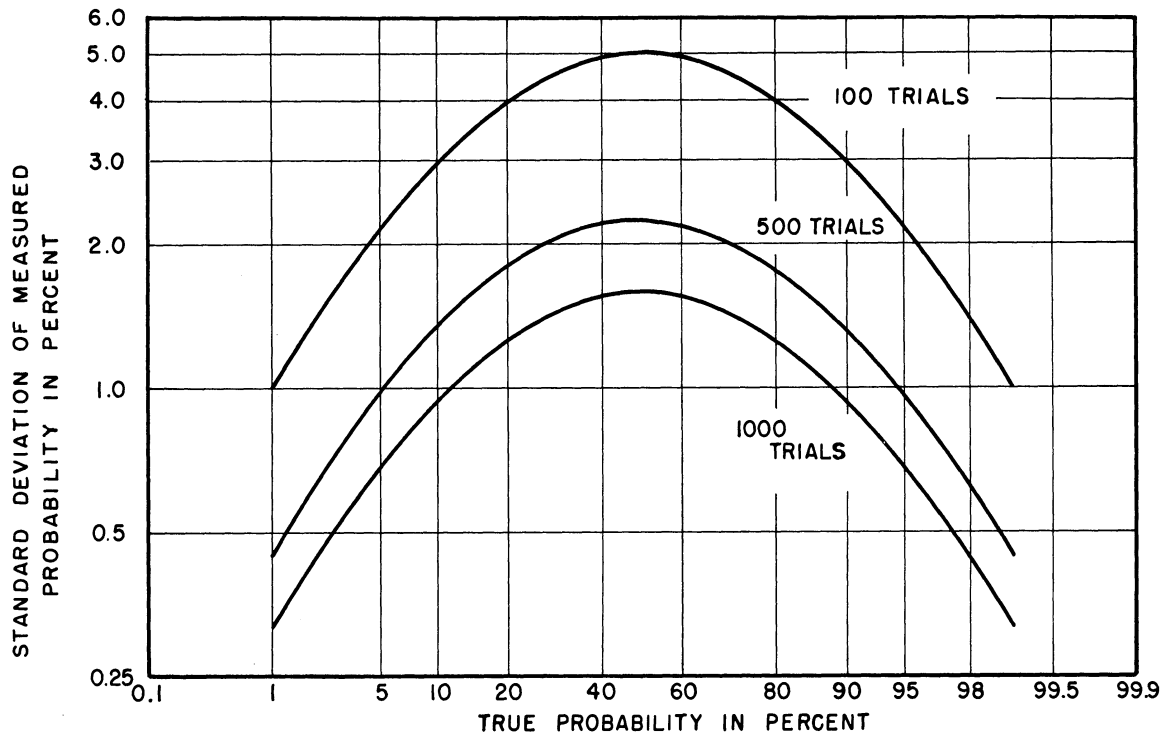


Fig. 5. Standard deviation of measured probability.

percentage error (ratio of ordinate and abscissa) of the measurement increases considerably as the true probability becomes small. To obtain reasonable statistical accuracy over the practical range of probability estimates, 500 trials or more should be taken.

The range of the operational amplifiers and discriminator circuits in SIMRAR is 60 volts. The receiver simulation must be scaled to comply with this restriction. It is also desirable to scale the simulation to use as much of the discriminator range as possible.

In using the recording circuits, the procedure is to preset the threshold levels of the discriminators according to the expected distribution of amplitudes. In general, this requires a known voltage level for each threshold. A convenient method of obtaining the settings is to use as input to the discriminators a known dc voltage equal to a desired threshold level. (This may be obtained from the voltage divider in SIMRAR.) Then, starting with a very high threshold, reduce

the threshold level until the counter records on every trial. This must, of course, be done for each discriminator to achieve different levels.

In signal detection studies, however, it is usually unnecessary to know the voltage level of each threshold. Rather, one frequently desires to achieve the widest range of false alarm probability for which the corresponding estimates of detection probability are meaningful data. The problem here is that the number of false alarms ("mistakes") falls off sharply as the detection performance improves. If the performance is exceedingly good, a very large number of trials is necessary to get a reasonably small percentage error in the false alarm probability estimate. In order to obtain data in a convenient length of time, the receiver performance must be restricted to be poorer than that characterized by about 96 percent detection at 2 percent false alarm.

4. COMPONENT CIRCUITS OF SIMRAR

4.1 Counter Chassis

The counter chassis of SIMRAR may be used, exclusive of the receiver simulator, as a statistical measuring device. The counter chassis houses 9 amplitude discriminator circuits, 18 counters (one pair for each discriminator), and the threshold potentiometers. In addition to the 9 discriminator circuits on the counter chassis, another identical circuit (No. 10) is included on the control chassis.

Figure 6 is the schematic diagram of the amplitude discriminator circuits. The input range of the discriminators is from 0 to 60 volts, positive only. The 6AB4 circuit is a cathode follower for isolation purposes. The 12AY7 and its associated circuitry form an

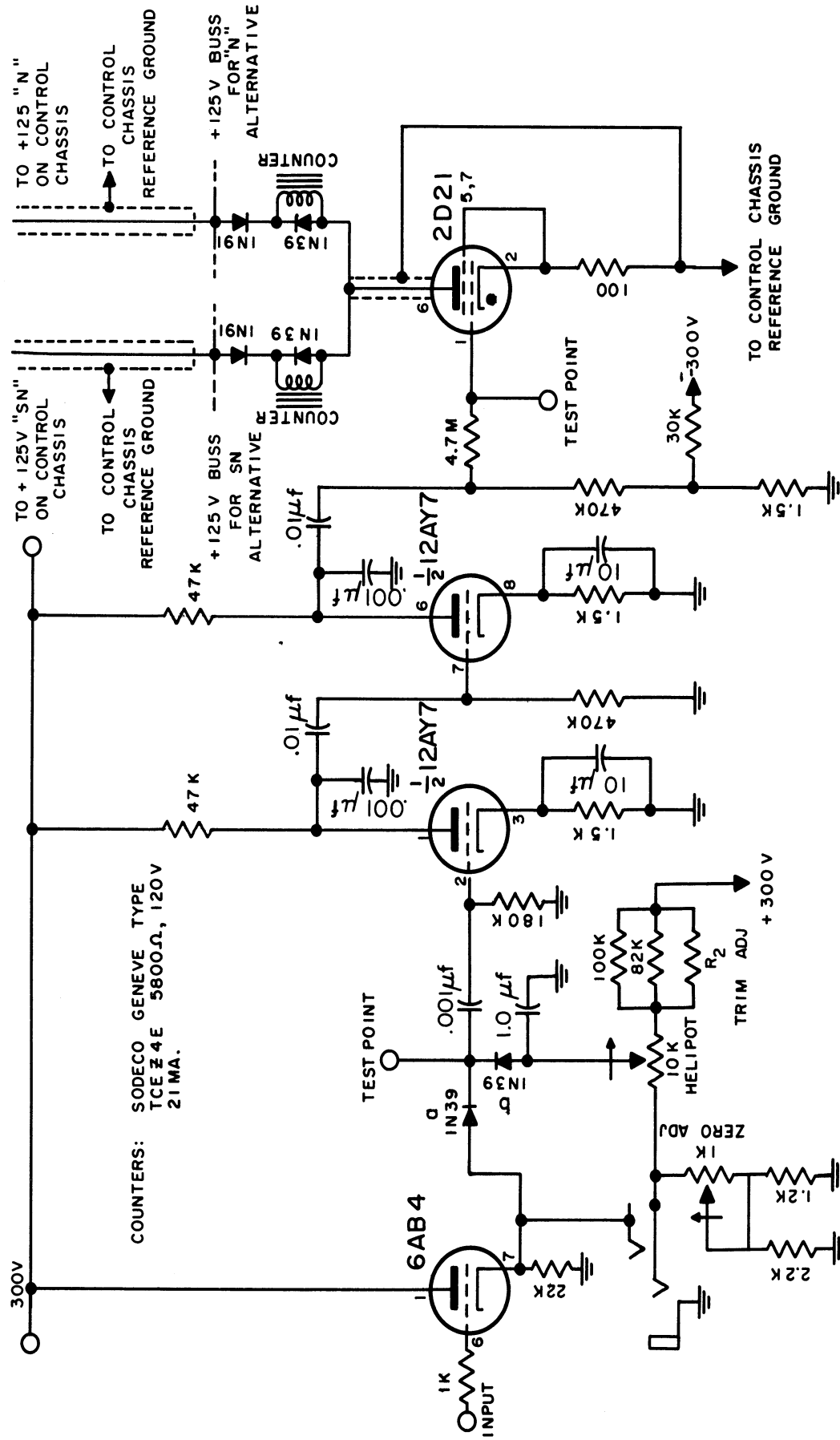


Fig. 6. Amplitude discriminator.

RC coupled bandpass amplifier tuned at approximately 2 kc. The 2D21 thyatron, when triggered from the 12AY7, draws sufficient current to operate the counters.

The input signals to the amplitude discriminators are required to have added to them a 2 kc perturbation signal of about 100 millivolts peak amplitude. The presence of this signal allows accurate recording regardless of the slope with which the input crosses the threshold. The 2 kc signal, which has a distorted sinusoidal waveshape, is generated in an oscillator circuit on the control chassis. The oscillator output at the plate is about 120 volts, peak-to-peak. With proper resistances, amplifier No. 3 can be used as a summing amplifier to add the correct amplitude of the perturbation signal to the discriminator input.

The diode circuit at the grid of the first half of the 12AY7 essentially gates the 2 kc perturbation signal into the bandpass amplifier when the input signal exceeds the threshold value set on the 10K Helipot (threshold potentiometer). The RC circuit directly coupled to the grid has a very short time constant, and prevents any dc voltage from appearing on the grid. Thus, when the input voltage, as it appears at the cathode follower output, is less than the voltage at the Helipot pickoff, the voltage at the diode junction test point is the threshold voltage. The grid of the 12AY7 (first half) is at ground. The thyatron is biased to cutoff from a voltage divider on the -300 volt supply.

When the input voltage rises above the threshold level, diode "a" conducts and diode "b" is cutoff. The 2 kc perturbation signal riding on the input signal is amplified through the bandpass

amplifier, and brings the thyatron grid voltage up to where the thyatron fires, operating the counter. The proper counter for recording is selected, according to the alternative in progress, by the control circuit which applies +125 volts to the proper terminal of the discriminator circuits.

The phase of the 2 kc/s perturbation signal will be random at the instant the input crosses the threshold level. In order for recording to occur, the input must be above the threshold long enough to allow at least one full cycle of the perturbation signal to go through the amplifier. Figure 7 is the frequency response curve for the No. 10 amplitude discriminator amplifier. The bandwidth of the amplifier is 4.24 kc/s, and, hence, one cycle of the 2 kc/s signal should always be sufficient to trigger the thyatron. Thus the discriminator input should be band-limited below 2 kc/s. The response curves for other channels

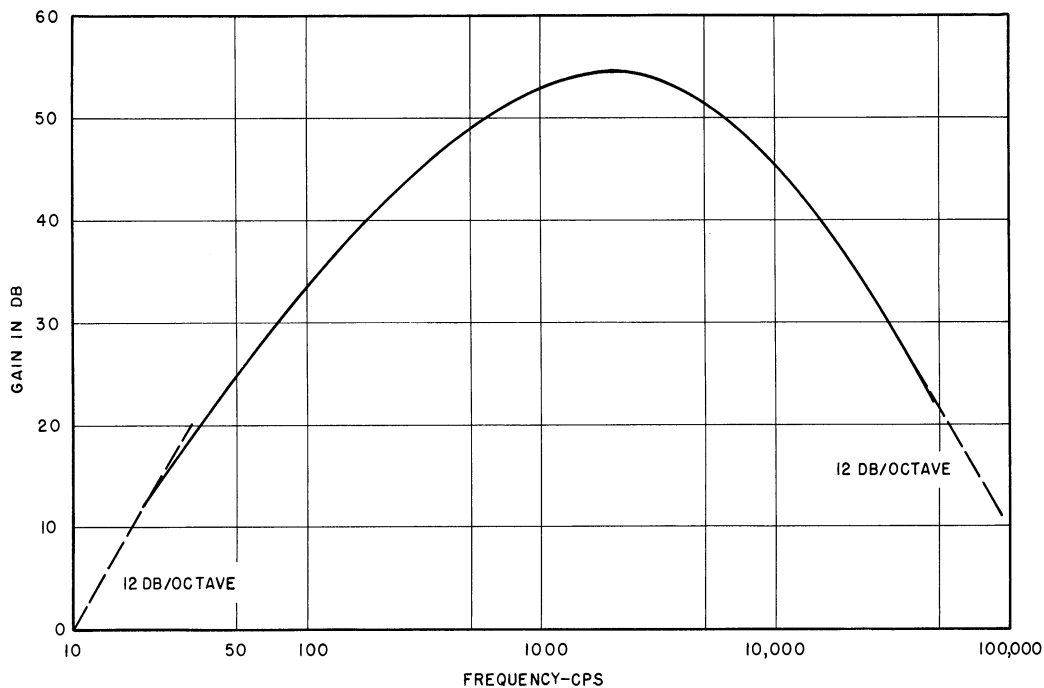


Fig. 7. Gain-frequency response of discriminator amplifier.

may differ slightly from Fig. 7 due to variation in the individual component values from the nominal.

The amplitude discriminators may be zeroed as follows: run the threshold potentiometer down to zero, and apply only the perturbation signal at the input. Then the zeroing pot is adjusted, with the properly scaled perturbation signal at the discriminator input, so that no counts occur. Alternatively, meter jacks are provided on the front panel so that an ammeter may be used.

Figures 8 and 9 are front and rear views of the counter chassis, pointing out significant features of the circuits.

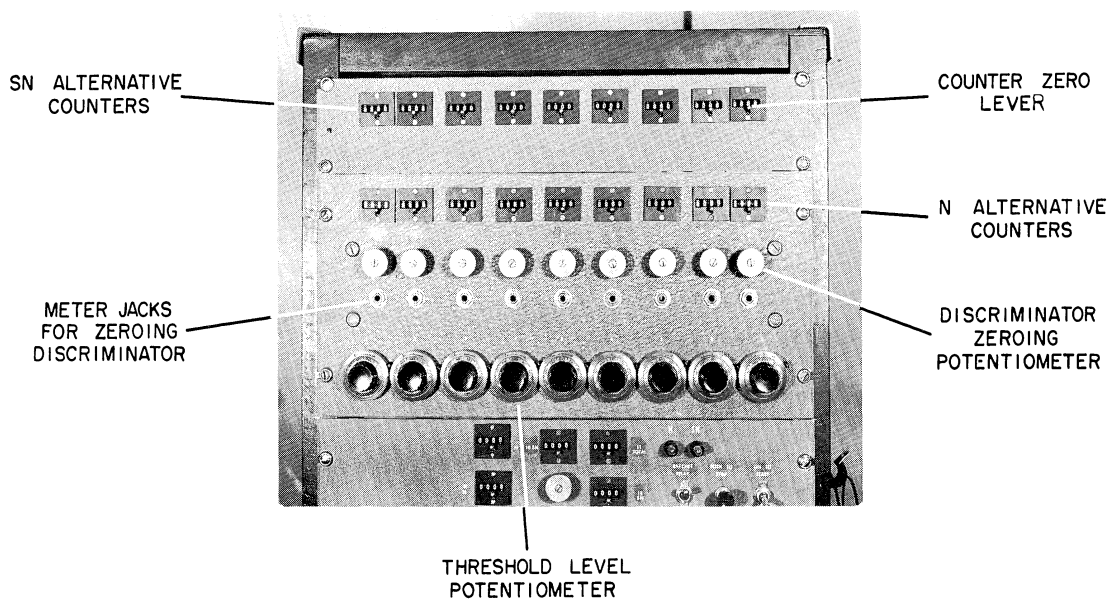


Fig. 8. Front view of counter chassis.

4.2 Control Chassis

4.2.1 General Description. The control chassis is comprised of the timing wave generator, the control circuit which performs the switching functions to reset SIMRAR for the next trial, the 2-kc perturbation voltage oscillator, and operational amplifier No. 3. In addition, the No. 10 and No. 11 amplitude discriminators and associated counters

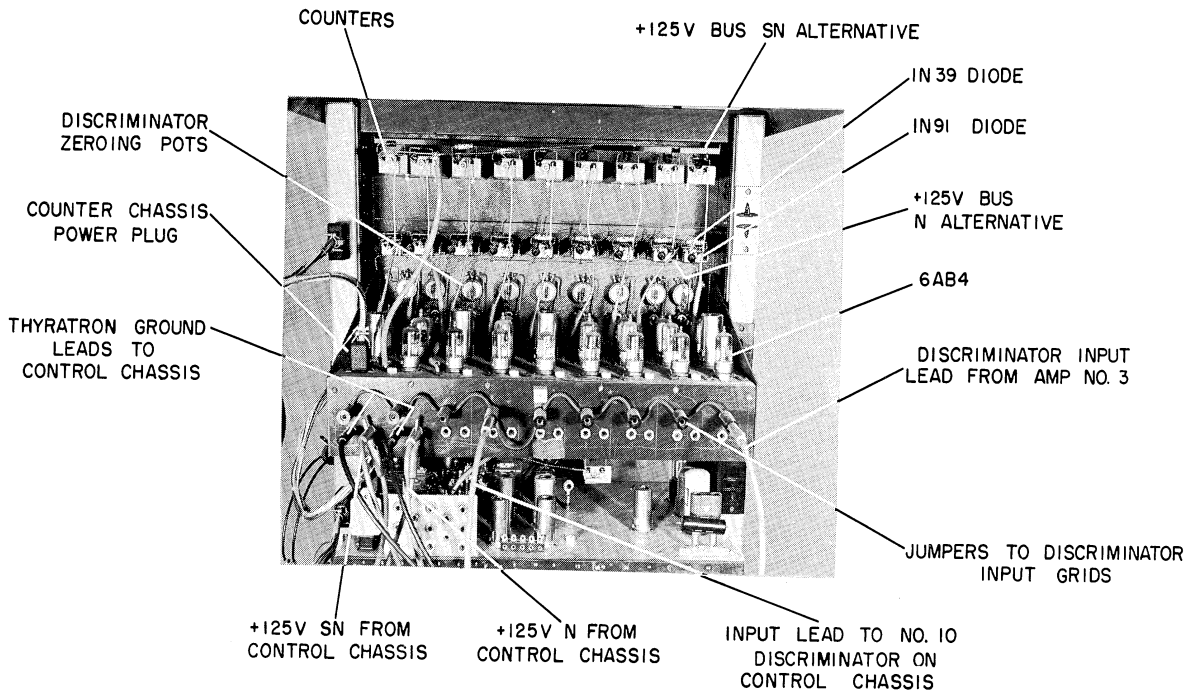


Fig. 9. Rear view of counter chassis.

are on the control chassis.

Figures 10 and 11 are front and top views of the control chassis, pointing out the positions of relays and other components. The back of the control chassis is made into a plug board, on which various

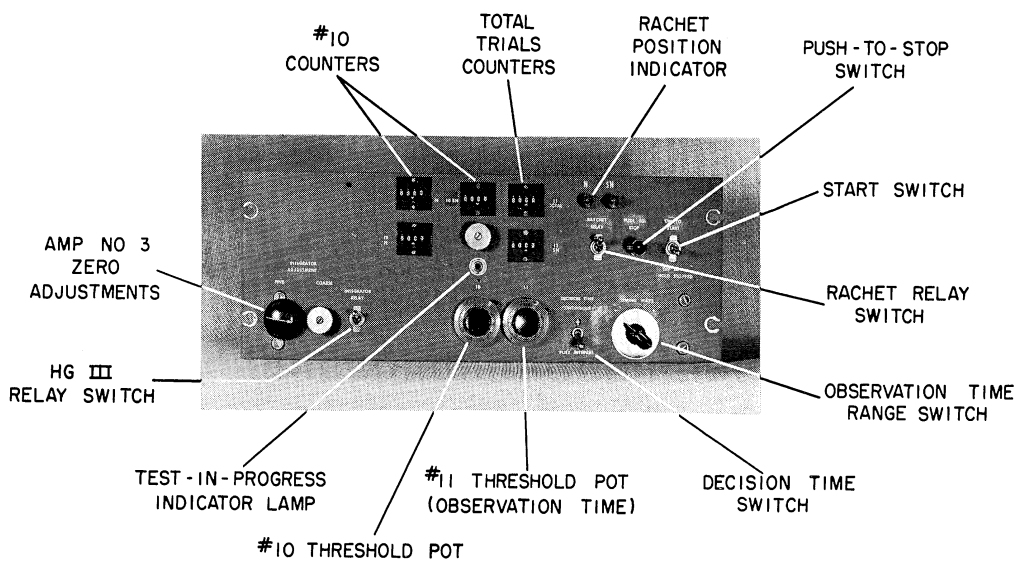


Fig. 10. Front view of control chassis.

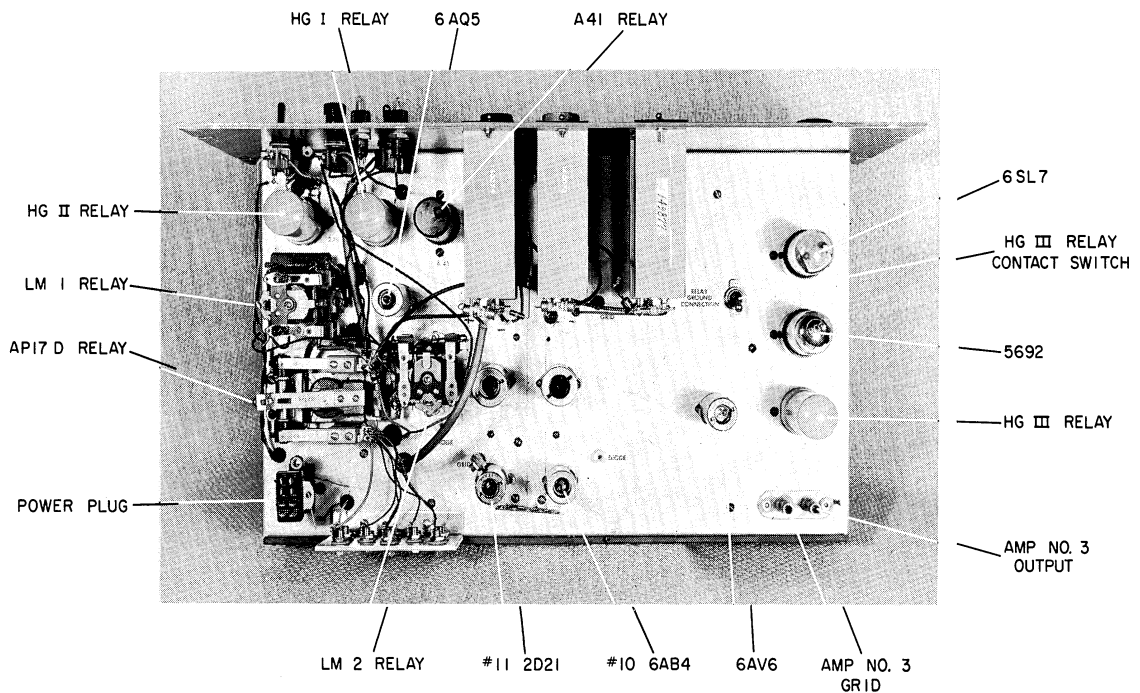


Fig. 11. Top view of control chassis.

test points and circuit terminals are available for testing and operational convenience. Figure 12 is a diagram of this plugboard. Table II describes the connections to the various jacks.

4.2.2 Timing Control. Control of the observation time of SIMRAR is usually achieved through the No. 11 amplitude discriminator which is

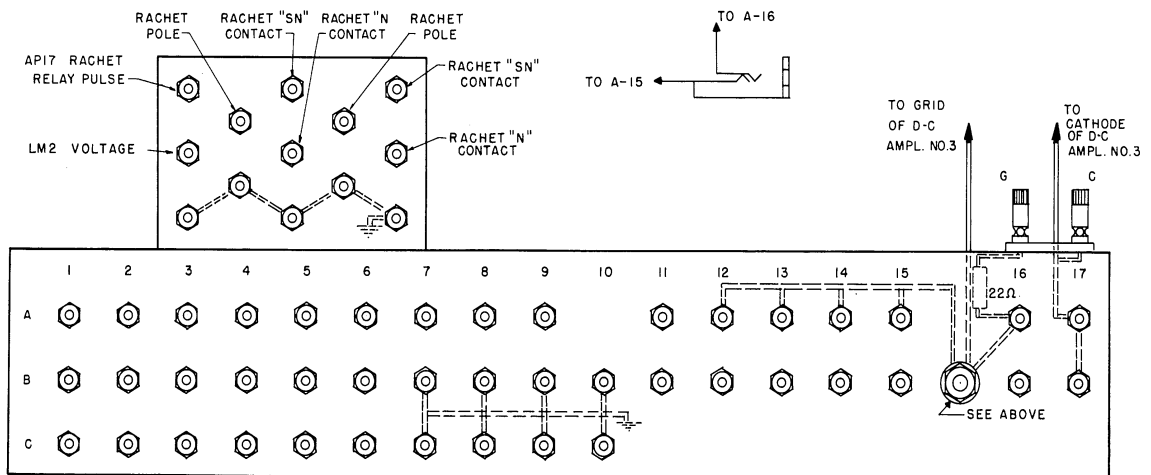


Fig. 12. Control chassis plugboard connections.

TABLE II

CONTROL CHASSIS PLUGBOARD CONNECTIONS

	A	B	C
1	HG I relay contact 2 through 120 k	HGI relay contact 2	No connection
2	+125 volts SN alternative	+125 volts N alternative	No connection
3	IM 2 relay contact K	Push to stop switch contact	6AQ5 grid-pulse to preset counter
4	No. 10 2D21 plate	No. 11 2D21 plate	No connection
5	Control circuit termination supply	No. 10 plate SN alternative	No connection
6	No. 11 plate	No. 10 plate No alternative	No connection
7	No. 11 discriminator input	Ground	Ground
8	Timing wave generator output	Ground	Ground
9	No. 10 discriminator input	Ground	Ground
10	No connection	Ground	Ground
11	6AQ5 plate	No. 11 2D21 grid	
12	Amp. 3 grid	No connection	
13	Amp. 3 grid	No connection	
14	Amp. 3 grid	No connection	
15	Amp. 3 grid	No connection	
16	Amp. 3 grid	2 kc oscillator output	
17	Amp. 3 cathode output	Amp. 3 cathode output	

connected externally to the termination supply of the control circuit. The test (detection trial) in progress is terminated when the 2D21 thyatron of the No. 11 discriminator fires.

Figure 13 is a schematic diagram of the timing wave generator and No. 11 discriminator. The No. 11 discriminator is similar to the other discriminator circuits, except that it operates only on negative inputs. The timing wave generator is a simple capacitor charging network, with a selection of three relatively large time constants available. A nearly linear sawtooth of either positive or negative polarity can be obtained by proper setting of the selector switch. The proper 2-kc perturbation signal amplitude is added internally to the timing wave.

In fixed time tests, the negative timing wave (positions 1 through 3 of the selector switch) is externally jumpered to the input of the No. 11 amplitude discriminator. The threshold level adjustment of No. 11 then provides a continuous variation of observation time within the range selected. The total range available is 30 msec to 3.5 seconds. In sequential tests, it is desired to observe the input to the decision device until the decision can be made with a chosen probability of error. The distribution of decision time is then measured. Hence, for this case, the input to the No. 11 discriminator is the decision function (receiver output), and the positive timing wave (positions 4 through 6 of the timing wave selector switch) is applied to the other discriminator circuits in the counter chassis.

Now, using No. 11 discriminator, a test will be terminated by a negative input (negative timing wave, or negative decision function). The No. 10 discriminator is also available through external connections

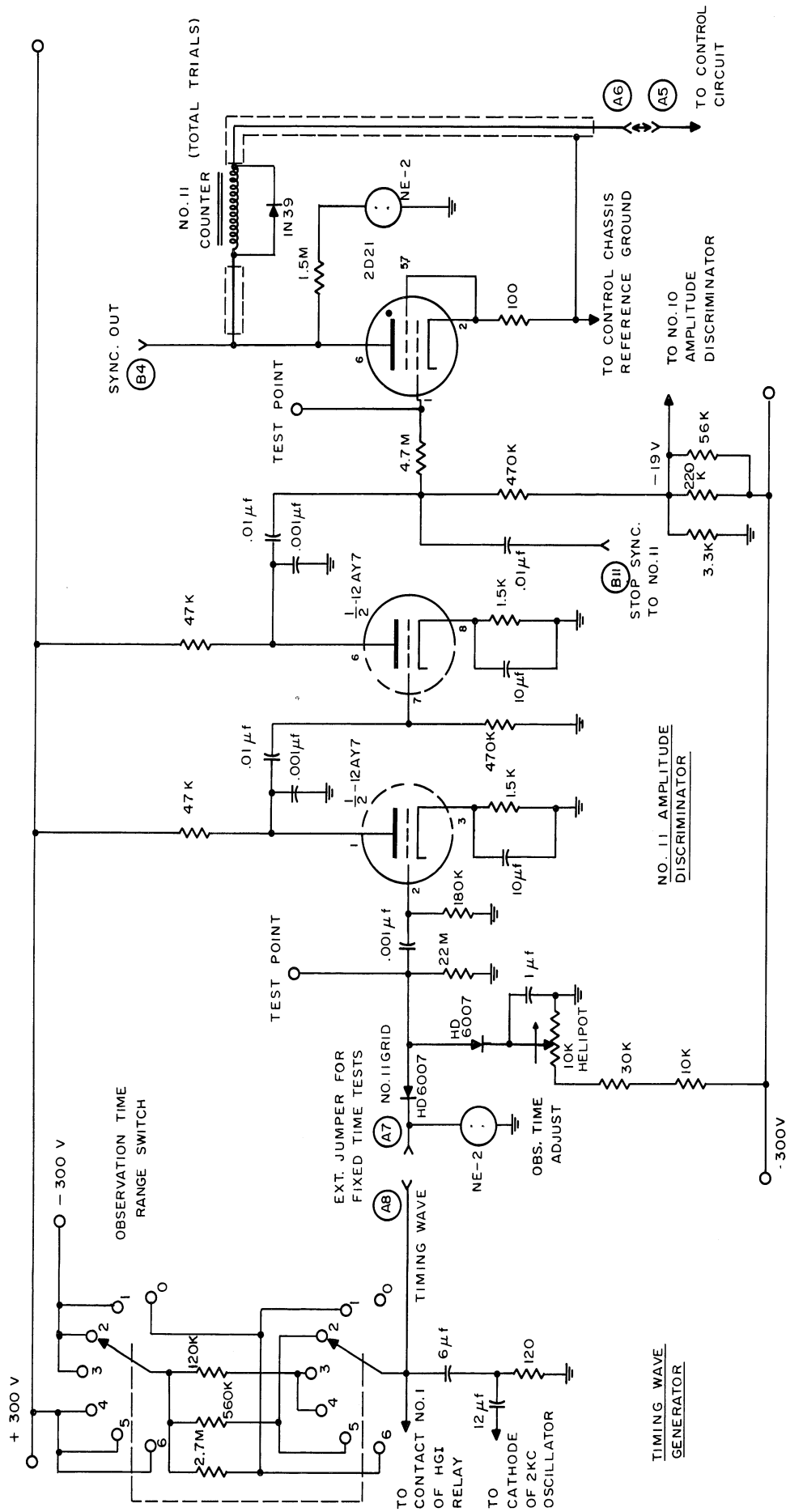


Fig. 13. SIMRAR timing control.

on the control chassis, and could be used for test termination with positive inputs. Using No. 10 and No. 11 in parallel as the cycling control circuit termination supply, the test can be terminated by an input which goes both positive and negative.

The NE-2 lamp off the plate of the No. 11 2D21 gives an indication of test in progress when the No. 11 discriminator is used as termination supply for the cycling control circuit.

SIMRAR timing may also be controlled from an external source through terminal B 11 on the plugboard.

4.2.3 Cycling Control Circuit. The cycling control circuit of SIMRAR performs the complex switching functions for resetting and cycling. Figure 14 is the schematic diagram of the control circuit.

Figure 15 helps to explain the switching functions which occur. With the power on, and the start switch off, only the HG I and HG III relays are energized. (The HG III relay actually may or may not be energized, depending upon the position of the integrator relay switch.) The HG III relay parallels amplifier No. 3, and grounds the amplifier output if it is energized. The HG I relay grounds the timing wave generator, and ungrounds the 6AQ5 grid circuit when it is energized. The 6AQ5 grid circuit charges, with about a 0.6-second time constant, to -45 volts, which is sufficient to cut off the 6AQ5. The 1N54 diode in the grid circuit limits the grid voltage to -45 volts.

When the start switch is turned on, the following sequence occurs:

- (1) +125 volts is applied through the LM 1 and A41 relay contacts to the LM 2 relay. The LM 2 relay operates, ungrounding contact K.

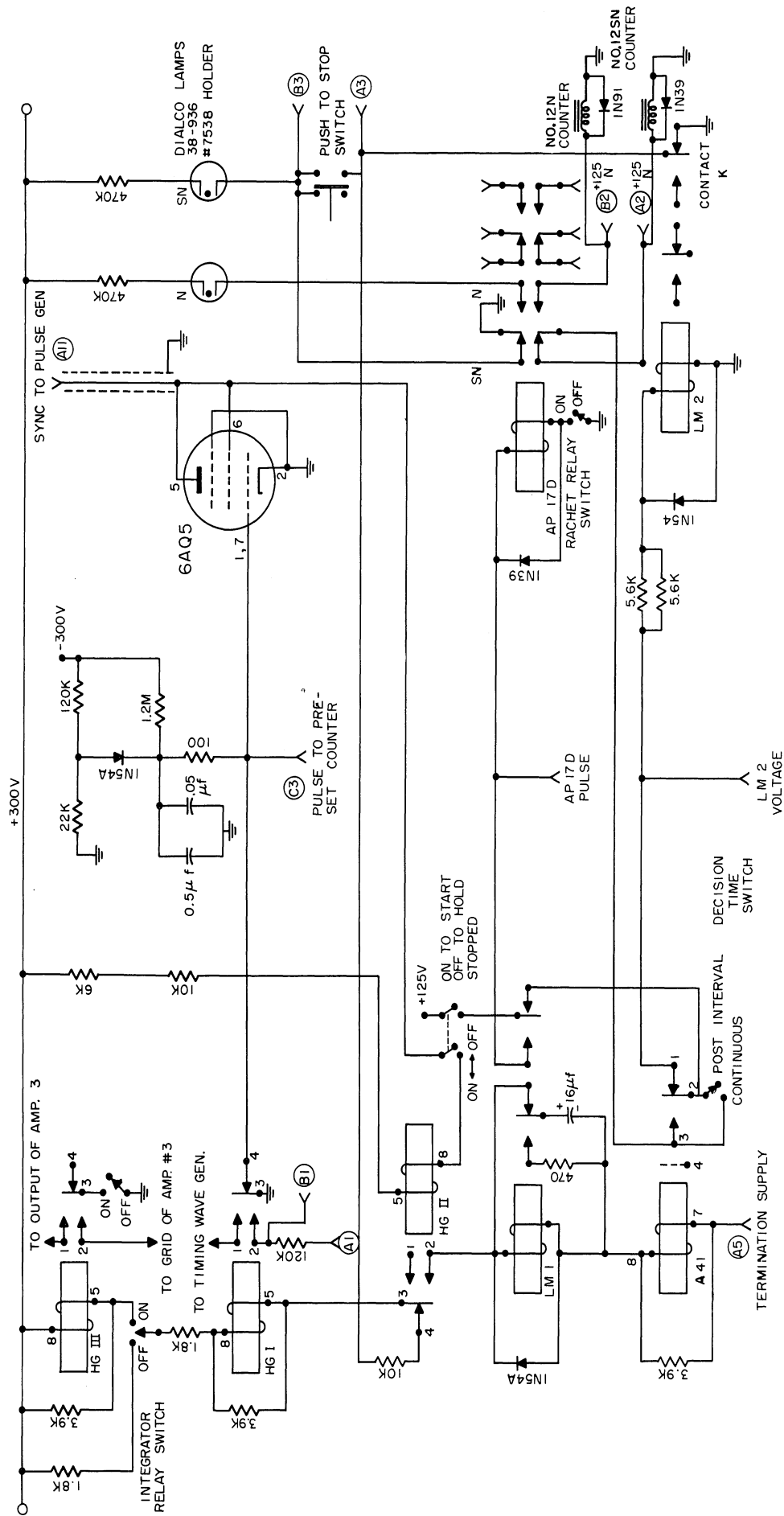


Fig. 14. Control circuit.

RELAY	MANUFACTURER	MFG. NO.	COIL RATING	COIL RES.
A 41	STEVENS - ARNOLD, INC.		30V 8MA	3800 Ω
LM 1	POTTER & BRUMFIELD	LM-11	6.3 MA	2500 Ω
LM 2	POTTER & BRUMFIELD	LM-11	6.3 MA	2500 Ω
LM 3	POTTER & BRUMFIELD	LM-11	110V	1250 Ω
AP 17 D	POTTER & BRUMFIELD	AP-17-D	6.6 MA	4000 Ω
HG 1	WESTERN ELECTRIC	275 C	6.6 MA	4000 Ω
HG 2	WESTERN ELECTRIC	275 C	6.6 MA	4000 Ω
HG 3	WESTERN ELECTRIC	275 C	6.6 MA	4000 Ω

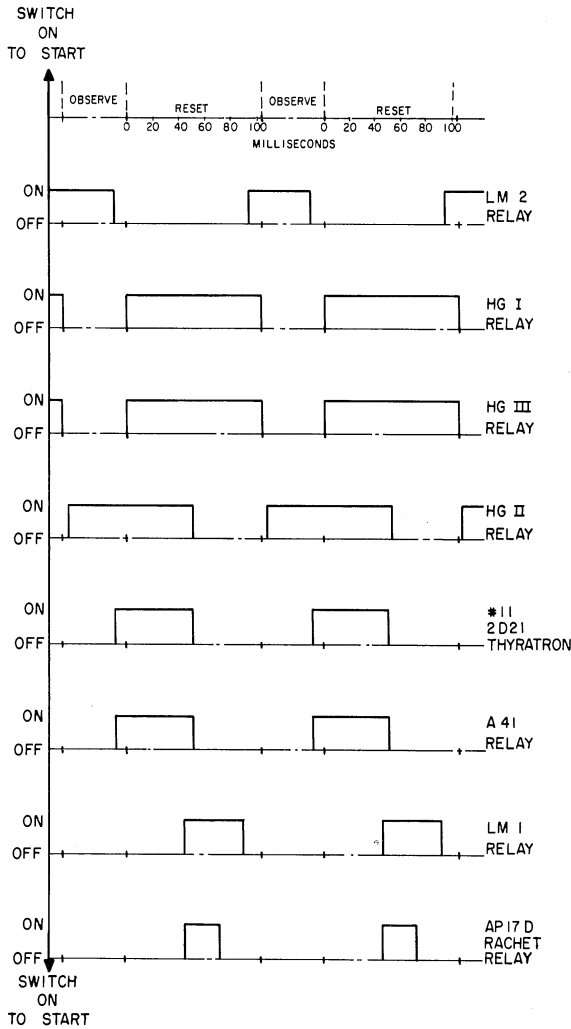


Fig. 15. Cycling control circuit relay sequence.

(2) When contact K opens, the HG I and HG III relays are de-energized. The observation interval begins.

(3) When the HG I relay opens, the timing wave starts, and the 6AQ5 grid is grounded. The 6AQ5 conducts, and HG II relay is energized.

(4) With the HG II relay energized, a conduction path exists from +300 volts through the HG I, LM 1, and A41 relays, providing conduction can occur through the termination supply. With the No. 11 discriminator as the termination supply, conduction does not occur until

the 2D21 thyatron fires. The thyatron fires when the timing wave (or decision function on sequential tests) exceeds the threshold level of the discriminator. The time interval between firing of the thyatron and transfer of the HG I contacts is approximately 9 milliseconds. When the HG I relay contacts close, the timing wave is grounded and the observation interval ends.

(5) The A41 relay operates when the 2D21 fires. With the decision interval switch open, +125 volts is applied to

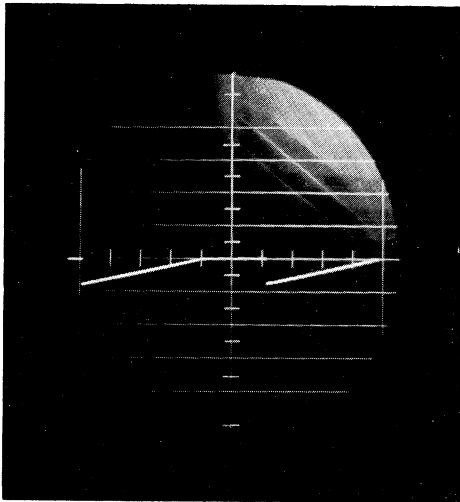


Fig. 16. Timing waveform (A8).
 20 v/cm vertical
 50 ms/cm horizontal

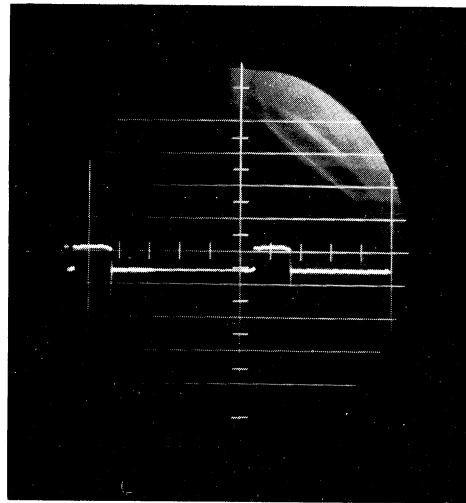


Fig. 17. #11 2D21 grid waveform.
 20 v/cm vertical
 50 ms/cm horizontal

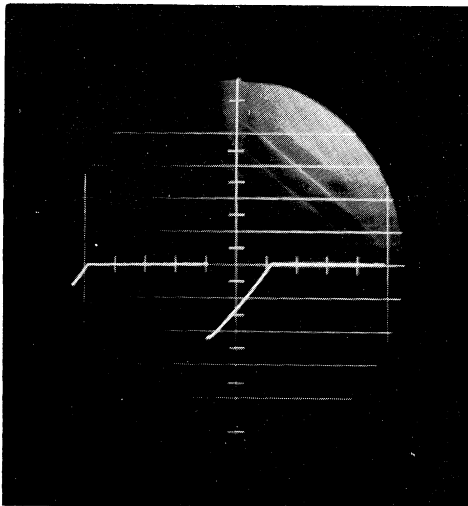


Fig. 18. 6AQ5 grid waveform (C3)
 20 v/cm vertical
 50 ms/cm horizontal

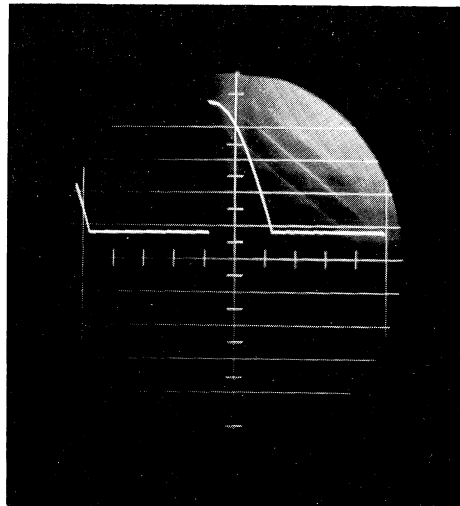


Fig. 19. 6AQ5 plate waveform (A11)
 60 v/cm vertical
 50 ms/cm horizontal

Note: In Figures 16 through 27, one centimeter is a large division on the grid. Do not scale the photographs.

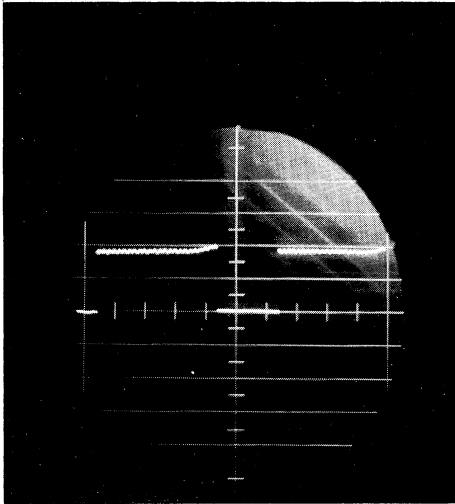


Fig. 20. LM2 relay voltage waveform.
60 v/cm vertical
50 ms/cm horizontal

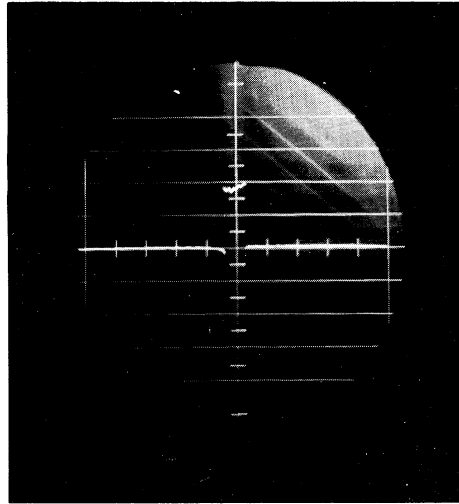


Fig. 21. AP17D pulse waveform.
60 v/cm vertical
50 ms/cm horizontal

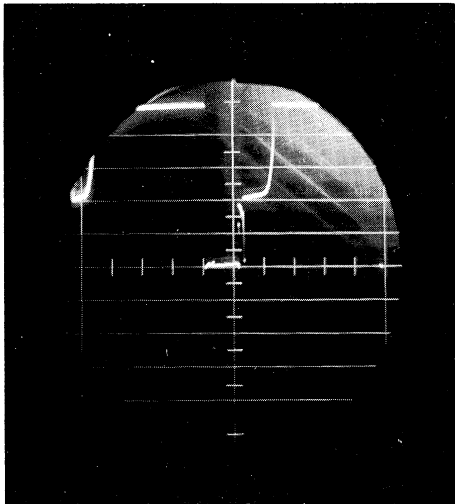


Fig. 22. Termination supply waveform.
60 v/cm vertical
50 ms/cm horizontal

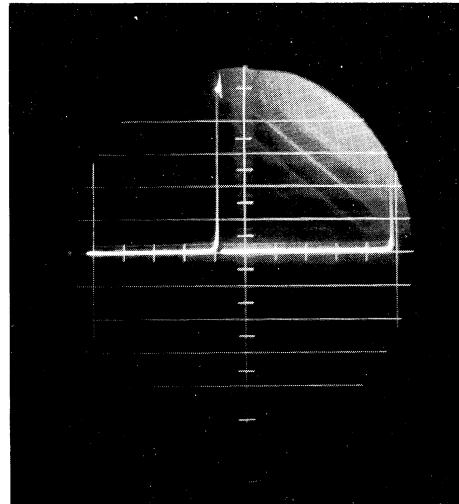


Fig. 23. Push-to-stop switch contact waveform (A3).
60 v/cm vertical
50 ms/cm horizontal

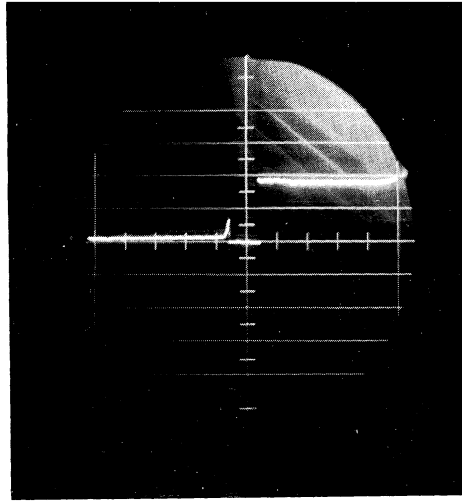
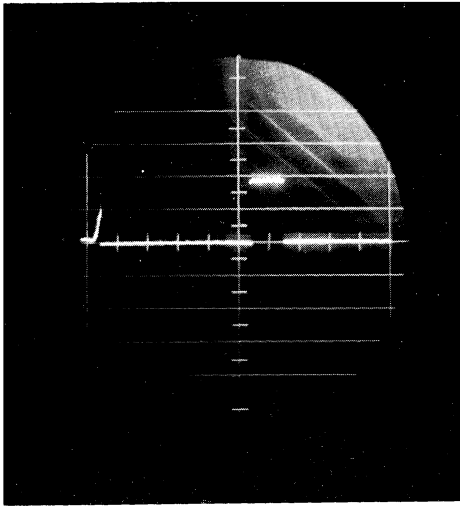


Fig. 24. +125 volts, SN-alternative
post-interval decision time (A2).
60 v/cm vertical
50 ms/cm horizontal

Fig. 25. +125 volts, SN-alternative,
continuous decision time (A2).
60 v/cm vertical
50 ms/cm horizontal

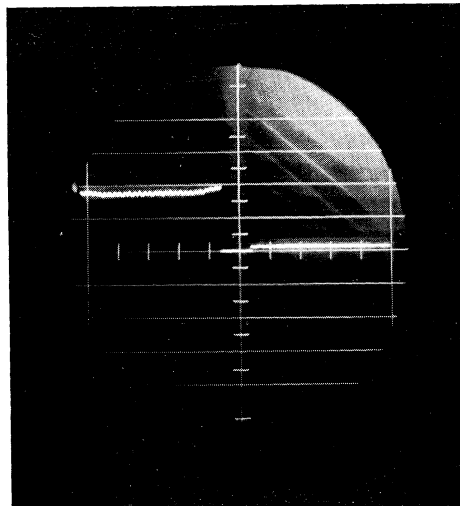
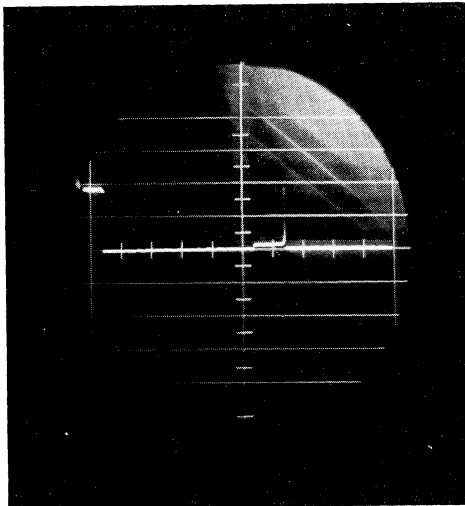


Fig. 26. +125 volts, N-alternative,
post-interval decision time (B2).
60 v/cm vertical
50 ms/cm horizontal

Fig. 27. +125 volts, N-alternative,
continuous decision time (B2).
60 v/cm vertical
50 ms/cm horizontal

the discriminator circuits in the counter chassis through the A41 relay contacts and the ratchet relay (AP17D) contacts. Hence, the post-interval decision corresponds to recording for the last 9 milliseconds of the observation interval. On continuous decision tests, the A41 relay is bypassed and +125 volts is applied to the discriminator circuits continuously during the observation interval.

- (6) The LM 1 relay operation is delayed approximately 50 milliseconds after firing of the 2D21. This is the time required for charging of the 16- μ f capacitor. When the LM 1 relay is energized, +125 volts is applied to the ratchet relay. The ratchet relay is an impulse relay, operating on pulses as short as 20 milliseconds. Operation of this relay switches the contacts from the SN or N positions to the other alternative, providing for transmission of the +125 volt recording power to the proper terminals in the counter chassis, and switching of the receiver simulation input.
- (7) When the A41 and LM 1 relays are de-energized, +125 volts is applied to the LM 2 relay, which operates and restarts the cycle.

Figures 16 through 27 are photographs of waveforms in the cycling control circuits extending over two consecutive observation intervals. The observation interval is about 0.2 second. The first interval, beginning at the right side of each photograph, is the SN alternative.

The A41 millisecond relay has a life of about three months under fairly constant use. Since this relay switches the +125 volt recording power to the counter chassis, arcing at the contacts will eventually cause them to stick together. A symptom of this failure is intermittent rapid cycling of the control circuit. The relay should be replaced when this occurs.

Cycling of the control circuit may be stopped by throwing the start switch to the off position, removing +125 volts from the control circuit. In this case, the cycling may cease with the ratchet relay in either of the SN or N positions. If the push-to-stop switch is used to first stop the cycling, and the start switch thrown off to hold stopped, the ratchet always stops in the SN position. This is a desirable mode of operation, since each series of trials will start on the same alternative (SN) and end after completion of an N alternative. Thus the same number of trials on each alternative is obtained.

The Dialco lamps give a visual indication of the position of the ratchet relay. If the experiments to be performed do not require switching of the ratchet position, the ratchet relay switch may be thrown to disengage the relay. In this case, recording will occur on only one bank of counters in the counter chassis.

The external availability of various control circuit voltages and relay contacts provides some versatility in the use of other equipment with SIMRAR. Terminals A1 and B1 on the control chassis make it possible to sync external equipment to the SIMRAR cycle through the HG I relay. Two additional sets of contacts are available on the ratchet relay, although one set would normally be used to switch the receiver input in the simulation. Also available on plugboard terminals

are the AP17D and LM 2 relay voltages, 6AQ5 plate and grid voltages, which may be used as triggers for external equipment.

The No. 12 counters record the number of trials on each alternative, operating directly from +125 volts through the ratchet relay contacts.

4.2.4 2 kc Perturbation Oscillator. Figure 28 is the schematic diagram of the 2-kc perturbation voltage oscillator. The distorted

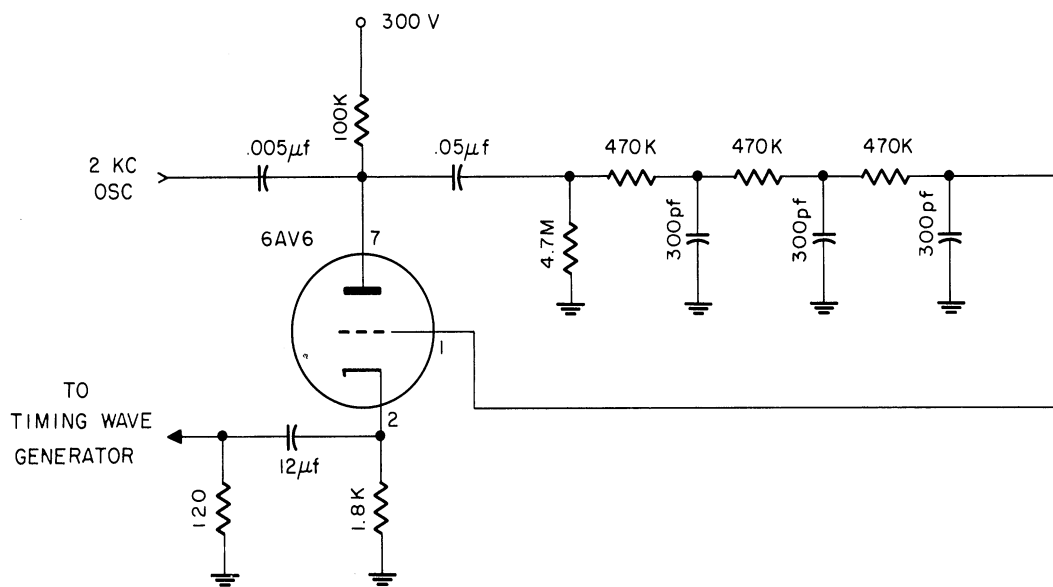


Fig. 28. 2 kc oscillator schematic.

sinusoidal signal obtained from this oscillator, shown in Fig. 29, is connected directly to the timing wave generator, and should be added with proper amplitude externally to the input to the recording circuits of SIMRAR. The signal therefore plays an important part in the timing and recording operation of SIMRAR.

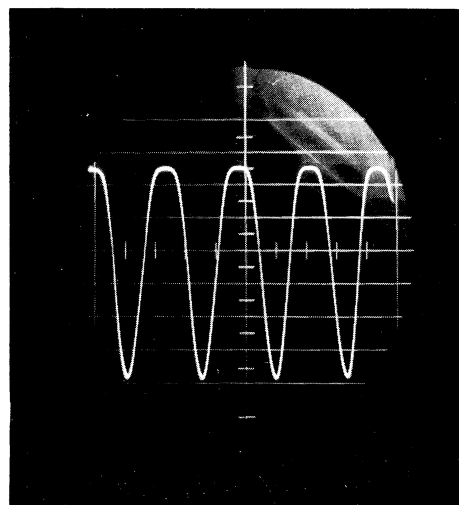


Fig. 29. 2 kc oscillator output waveform.
20 v/cm vertical
.165 ms/cm horizontal

The oscillator is a simple RC phase-shift triode oscillator circuit. The coupling network from plate to grid introduces sufficient phase lag that with the open loop gain prevailing the circuit is unstable and oscillates at approximately 2 kc.

4.2.5 Operation Amplifier 3. Figure 30 is the schematic diagram of operational amplifier 3, which is on the control chassis. This

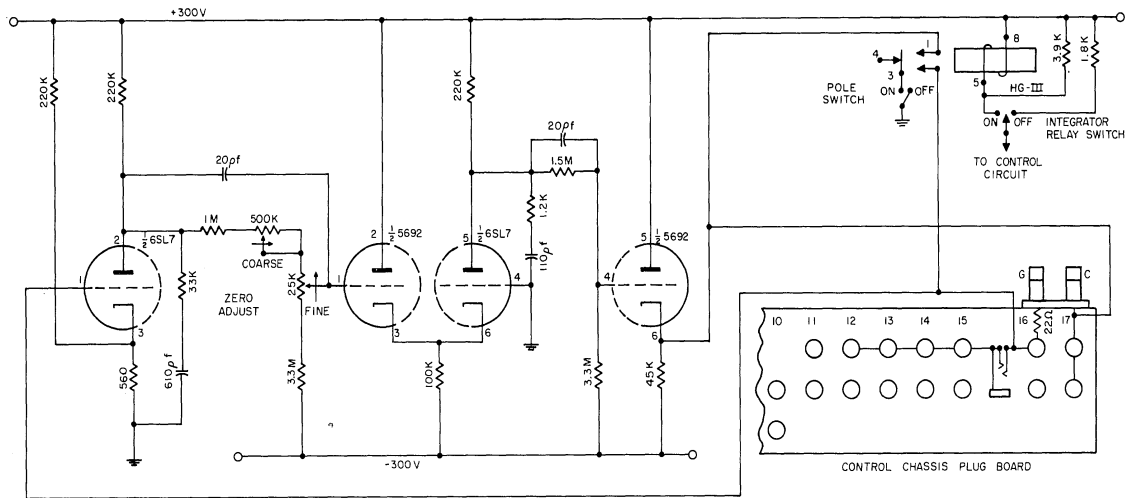


Fig. 30. Operational amplifier 3 schematic.

amplifier, as is typical of operational amplifiers, can be used as a summing amplifier, integrator, or general filter-amplifier with proper impedances in the input and feedback paths. Usually this amplifier is used in adding the perturbation signal to the recording head input. Hence, the output terminal of the 2-kc oscillator is physically close to the input of amplifier 3. In addition to an input terminal which is convenient for adding the 2-kc signal, there are four other input terminals. There are two output terminals. The terminals G and C are used for the feedback impedance.

The amplifier circuit utilizes a differential amplifier pair with a cathode follower output stage. Coarse and fine adjustments for

balancing the amplifier with zero volts input are provided. The amplifier gain, open loop, is +58 db, or a factor of 805. Figure 31 is the

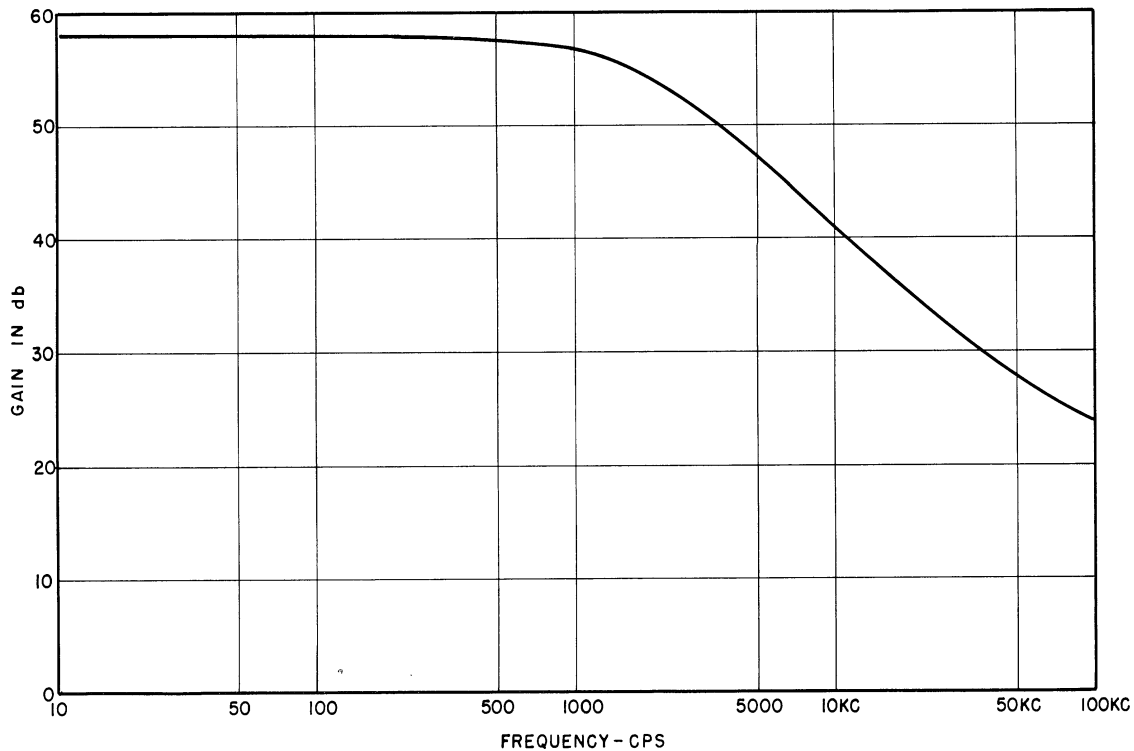


Fig. 31. Gain-frequency response of amplifier 3.

gain versus frequency characteristic of the amplifier.

With the integrator relay (so named because amplifier 3 is often used as an integrator) on, amplifier 3 can be used as a gated amplifier. When the observation interval is terminated, operation of the HG III relay in the cycling control circuit either grounds the amplifier output or shorts the input and output. In either case, the amplifier output is zero. In sequential tests, using both No. 10 and No. 11 discriminators as termination supply for the control circuit, the pole switch of the HG III relay should be "on" if the output of amplifier 3 can be larger than about 20 volts positive. This prevents a negative transient, which occurs when the relay contacts close from firing the No. 11 discriminator. In other cases, the switch can be "off."

It is important that replacement relays for the HG III be chosen so that contact 1 opens before contact 2. Otherwise, the plate dissipation of the output tube may be exceeded when the amplifier input is ungrounded with the output still grounded. About one out of three Western Electric 275C relays tested have this characteristic.

4.3 Main Simulator Chassis

4.3.1 Tuned Amplifier and Detector. Figure 32 is a front view

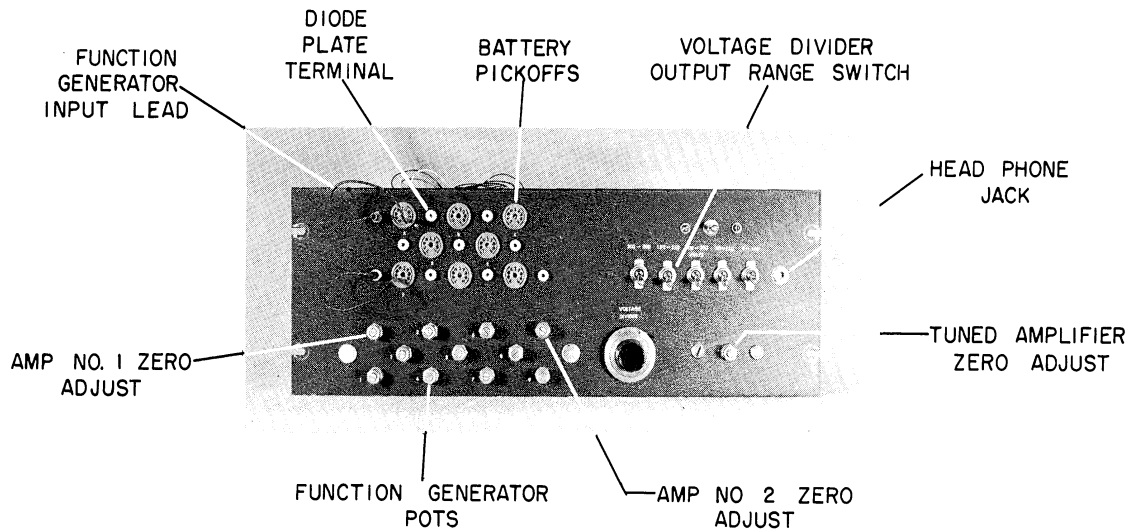


Fig. 32. Main simulator chassis, front view.

of the main chassis of the SIMRAR simulator. Figure 33 is a back view, showing primarily the tuned amplifier-detector chassis. Figure 34 is the schematic diagram of this circuit.

The tuned amplifier, which simulates the IF amplifier in a receiver simulation, is a two-stage circuit, with a choice of 10-kc or 1-kc center frequency. Each stage is a single tuned amplifier. On the 10-kc switch position, the first tuned stage has a resonant

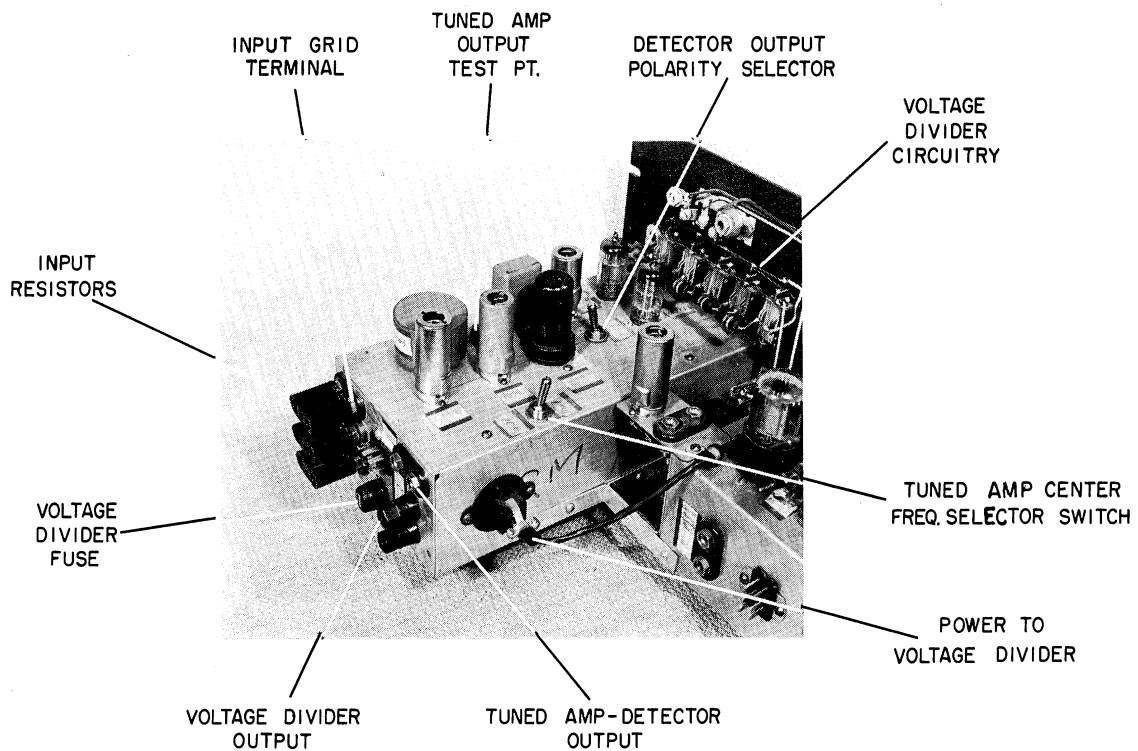


Fig. 33. Tuned amplifier-detector, back view.

frequency of about 10 kc, while the second stage has a resonant frequency of about 15 kc. Hence, the circuit is a stagger-tuned cascade on the 10-kc position. On the 1-kc position, both stages are tuned at 1 kc, hence the circuit is a synchronously-tuned cascade. Figures 35 and 36 are the gain versus frequency characteristics of the two tuned cascade circuits. The nominal total bandwidth of the 10-kc filter-amplifier is 400 cps, while the nominal total bandwidth of the 1-kc filter is 22 cps. In some detection problems it is necessary to know the equivalent noise bandwidth of the filter. By a graphical integration of the frequency response, it has been found that the equivalent noise bandwidth of the 1-kc filter is approximately 36.6 cps. The curves of Figs. 35 and 36 were obtained experimentally, and represent the gain from the input grid to the test point before the detector, including the loading effect of the 220-k

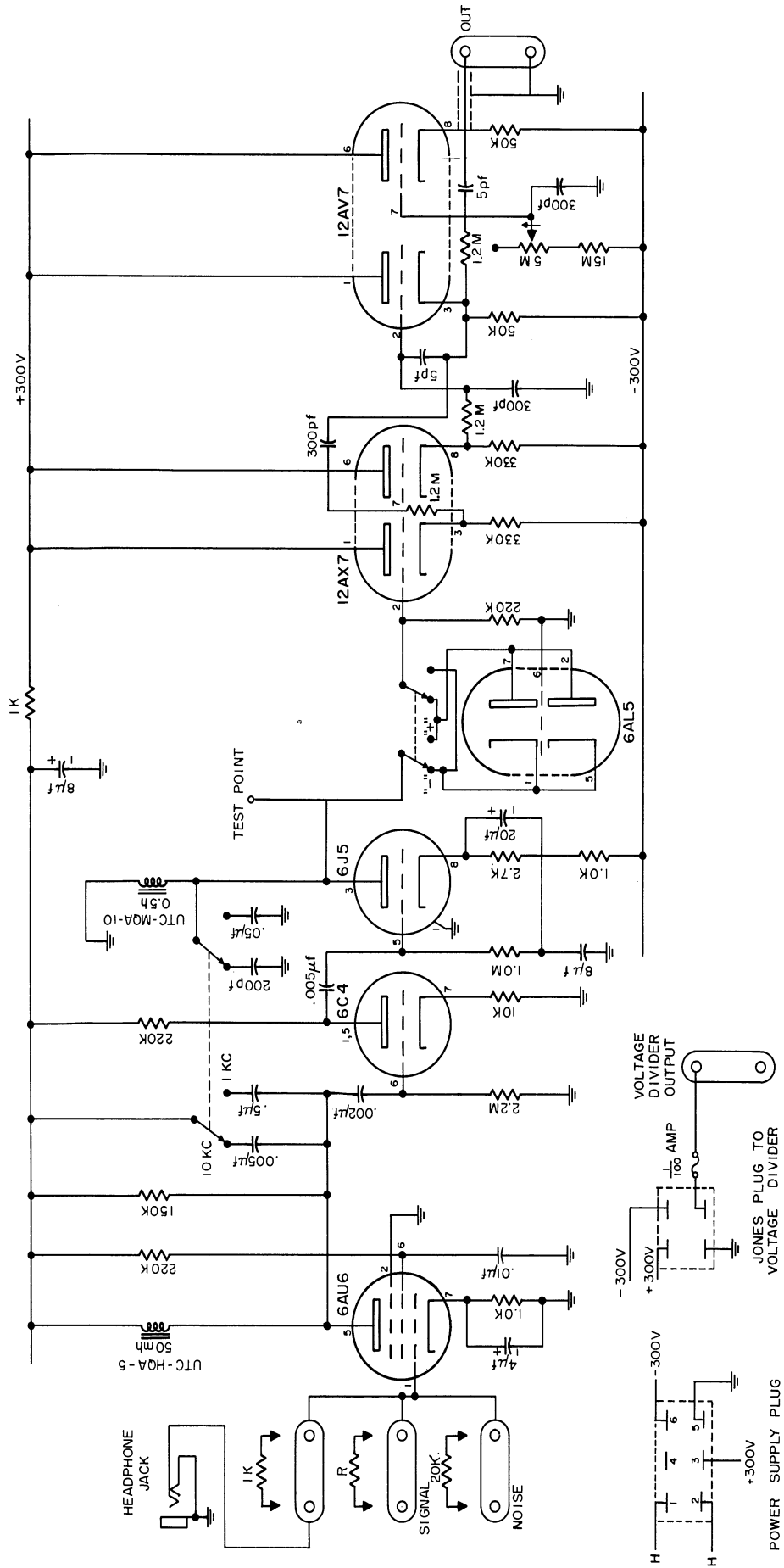


Fig. 34. Tuned amplifier and envelope detector.

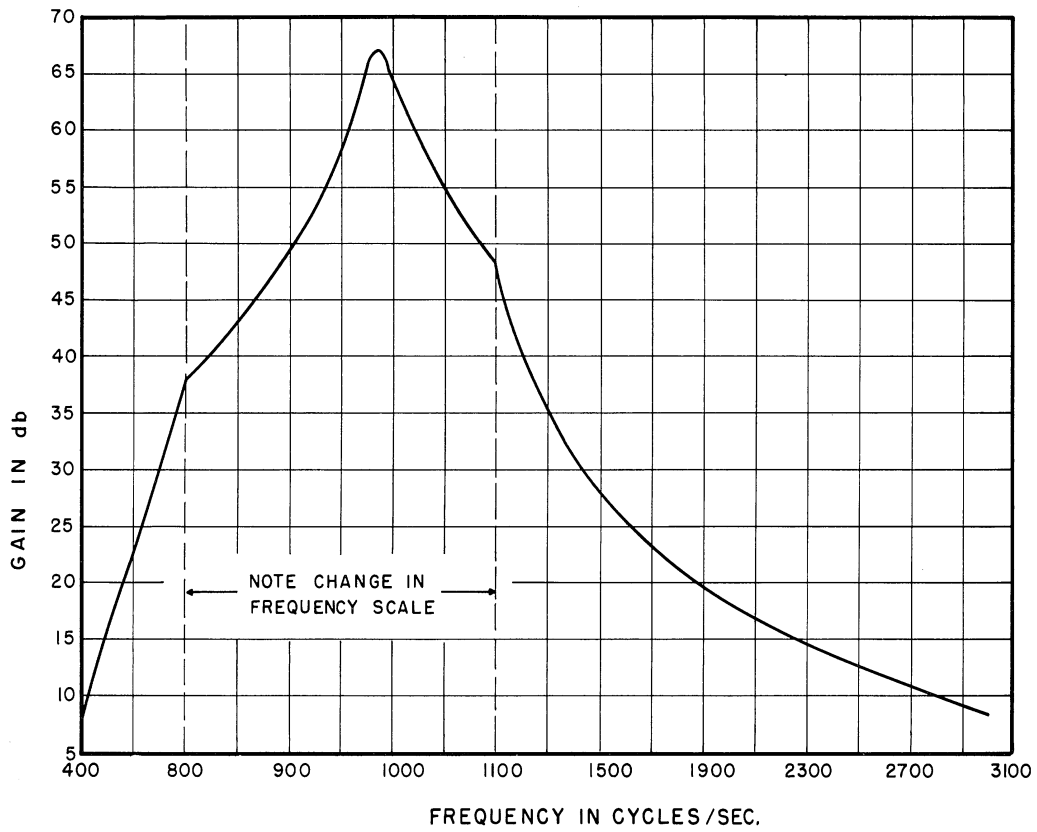


Fig. 35. SIMRAR 1 kc/s tuned amplifier; gain vs. frequency.

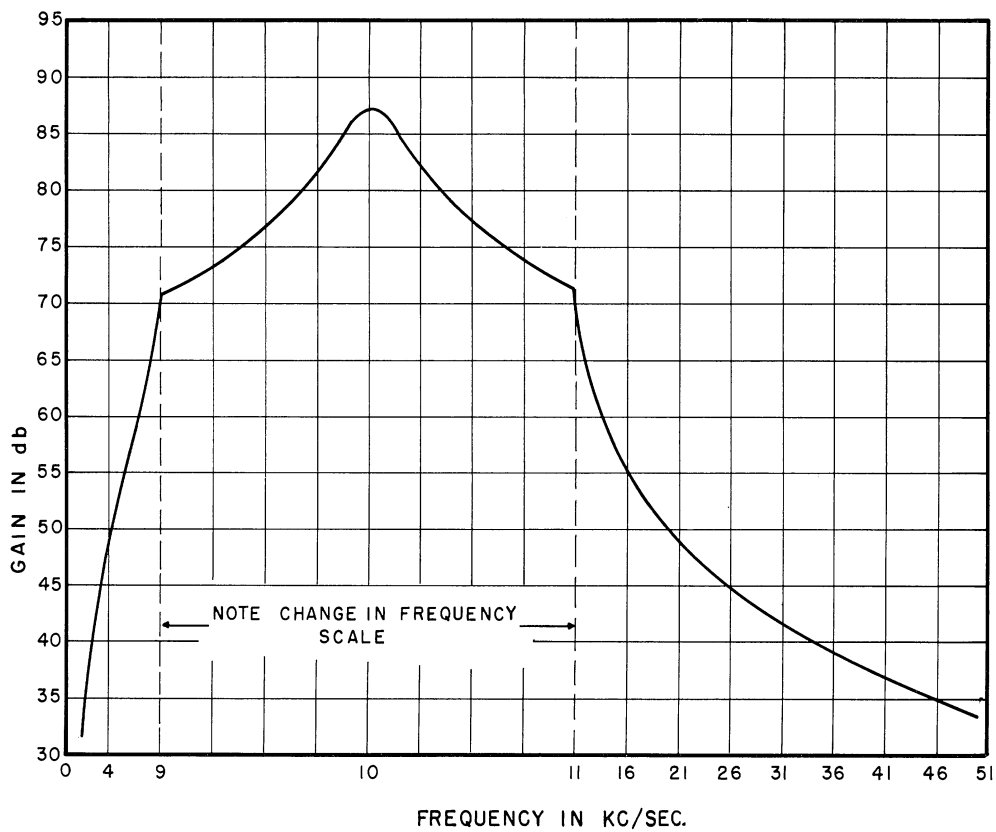


Fig. 36. SIMRAR 10 kc/s tuned amplifier; gain vs. frequency.

resistor at the detector output. In practice, the resistor network at the input grid introduces a considerable amount of attenuation. The gain from the point of actual signal input to the filter-amplifier output at the test point will differ from Figs. 35 and 36 by the amount of this attenuation.

The detector is a 6AL5 diode, which will pass the positive or negative half of the tuned amplifier output, according to the position of the selector switch. Since no sign inversion takes place after the detector, the output of the tuned amplifier-detector will have the same sign as selected on the switch. The 12AX7, 12AV7 circuits which follow the 6AL5 detector form a Butterworth 3-pole low-pass filter, with 400 cps bandwidth. This filter removes the "carrier" frequency from the detector output, giving the envelope of the tuned amplifier output. The frequency response of this wideband filter is shown in Fig. 37.

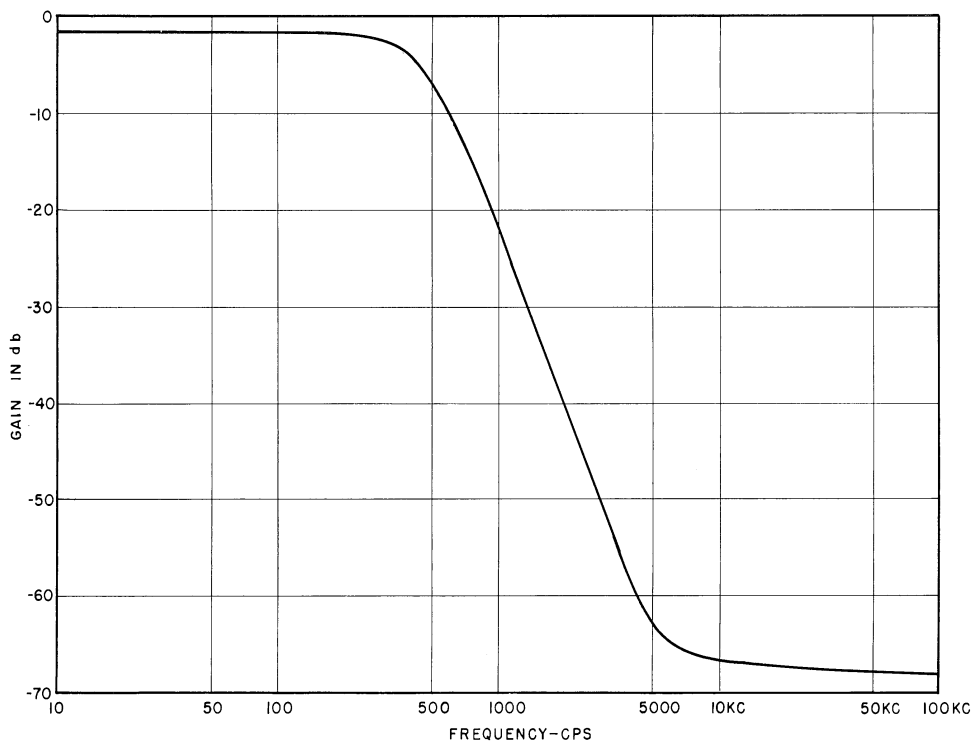


Fig. 37. Gain-frequency response of envelope detector filter.

4.3.2 Operational Amplifiers and Function Generator.

4.3.2.1 Circuit Description. Figure 38 is a back view of the amplifier-function generator chassis of the SIMRAR simulator.

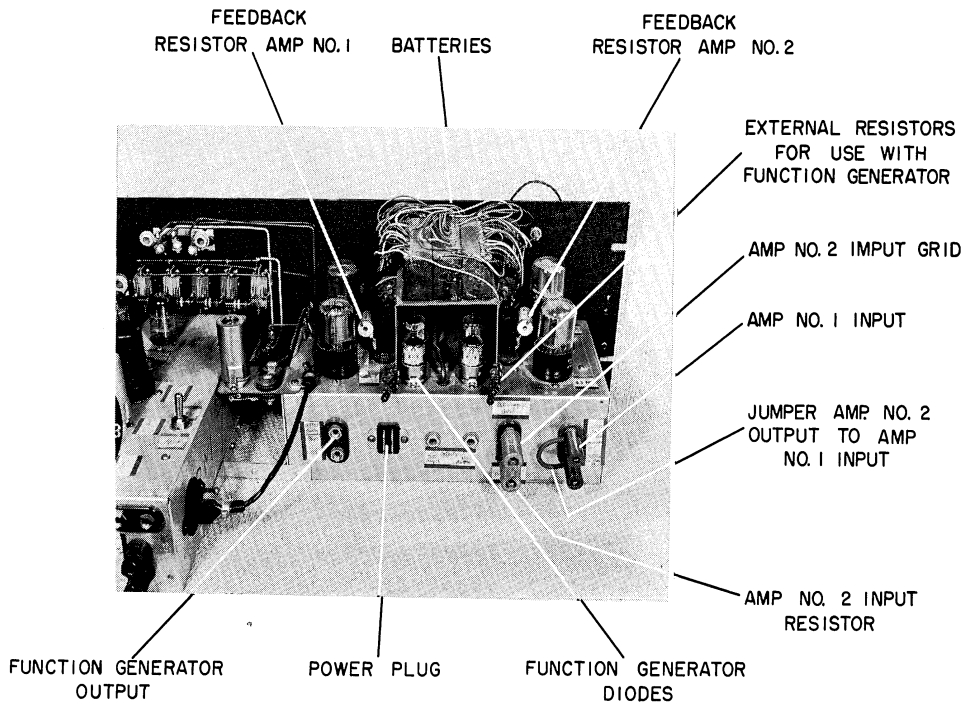
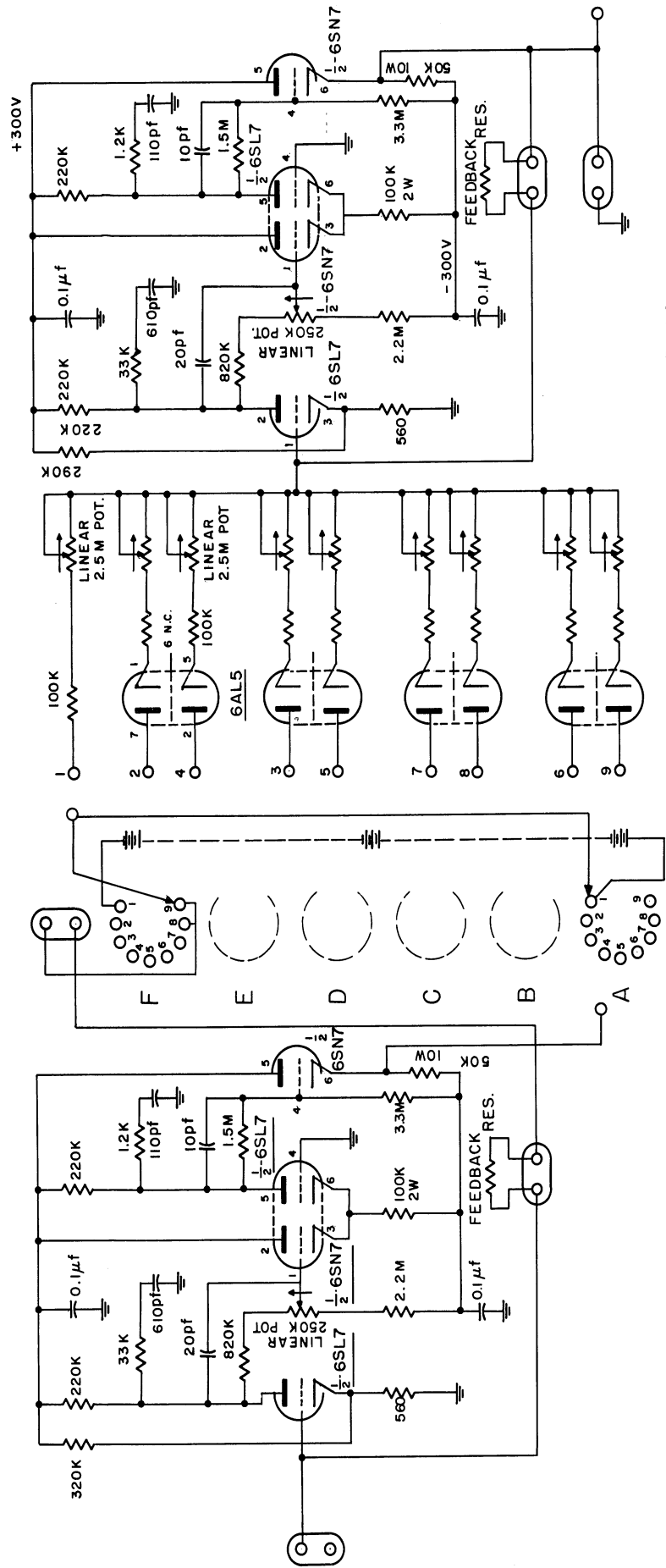


Fig. 38. Function generator, back view.

Figure 39 is the schematic diagram of the circuits.

Amplifier 2 can be used exclusive of the function generator to obtain required gain, and also filtering if proper input and feedback impedances are used. The amplifier circuit is very similar to that of amplifier 3 on the control chassis.

Since amplifier 2 is often used to obtain a required gain before the function generator, one output terminal of this amplifier is physically close to the function generator input terminal to facilitate external jumpering. The function generator and amplifier 1 must be considered as one circuit. The amplifier part of the circuit is identical



FUNCTION GENERATOR - AMPLIFIER NO. 1

AMPLIFIER NO. 2

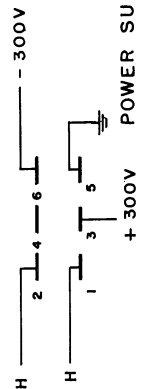


Fig. 39. Amplifier #2 and function generator.

to amplifier 2.

The function generator approximates a desired function by straight line segments. Nine segments can be used, one of which starts at zero input voltage. For this first segment, the function generator appears as a feedback amplifier, the gain of which can be adjusted by varying the input resistance to give a desired slope. The diodes are biased at the input voltage corresponding to the break points in the approximating function. Then, for all other segments, the function generator is a multiple adding amplifier. When the input exceeds the bias on the diode, the input is added with some adjustable gain to the total amplifier input which already exists. The adjustable gain determines the slope of the segment relative to the preceding one. A detailed explanation of setup procedure will be given in the next section.

The diode bias voltages are obtained from batteries. A range from 1.5 to 64.5 volts is available, in 1.5-volt increments. These voltages are brought to the front of the function generator panel on miniature tube sockets, the voltage increasing in the counterclockwise direction on the socket pins. The diode plates are brought out externally for setup purposes, and for this reason the input to the function generator must be of positive polarity. The positive terminal of the battery supply is connected externally in series with the input. When a diode plate is connected externally to a battery pickoff, the diode is back biased by the amount of the voltage pickoff. Thus, the diode plate voltage doesn't become positive until the input voltage exceeds the pick-off voltage.

4.3.2.2 Setup Procedure for Function Generator. The function generator-amplifier 1 circuit, as shown in Fig. 39, is limited

to simulation of functions having an increasing positive slope, as shown in Fig. 40. The input to the function generator must be positive,

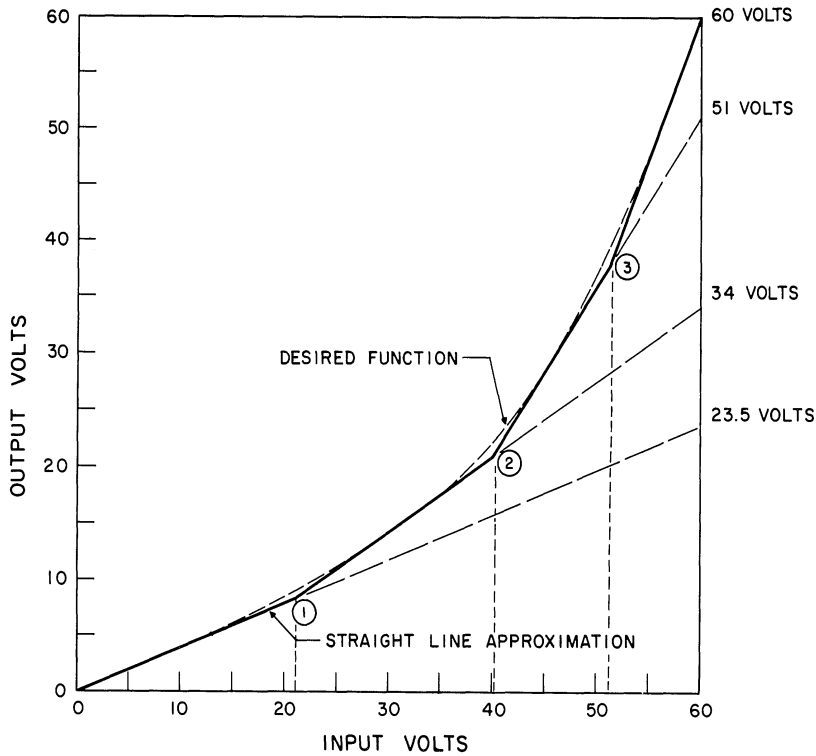


Fig. 40. An approximation to a function for simulation.

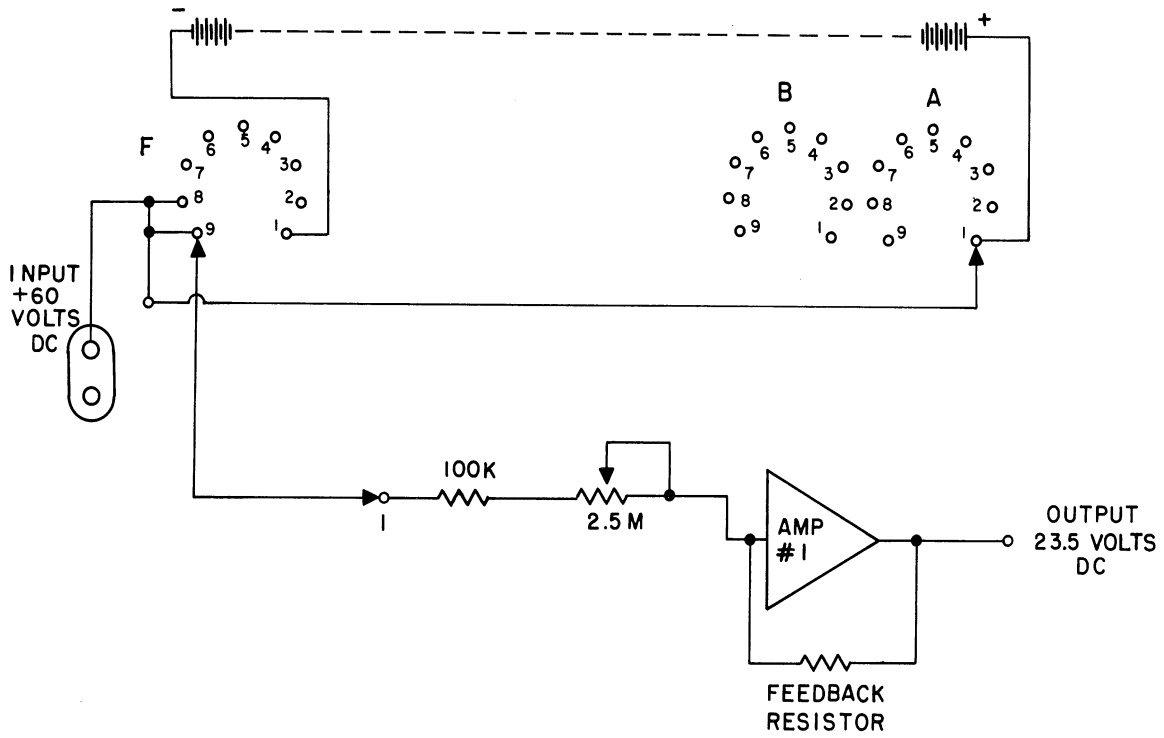
and since a sign reversal takes place in amplifier 1, the output will be negative. It is possible, however, using amplifiers 2 and 3 in addition to the function generator, to simulate functions having either increasing or decreasing slope (but not both), of either polarity. Simulation of functions, the slopes of which change sign, is not feasible with this equipment alone, unless the slope of one polarity is constant and changes abruptly to the opposite polarity.

Figure 40 illustrates a function which may readily be simulated with the function generator alone, and the straight line segment approximation to the desired function. (The sign reversal which takes place in amplifier 1 need not be considered in setting up

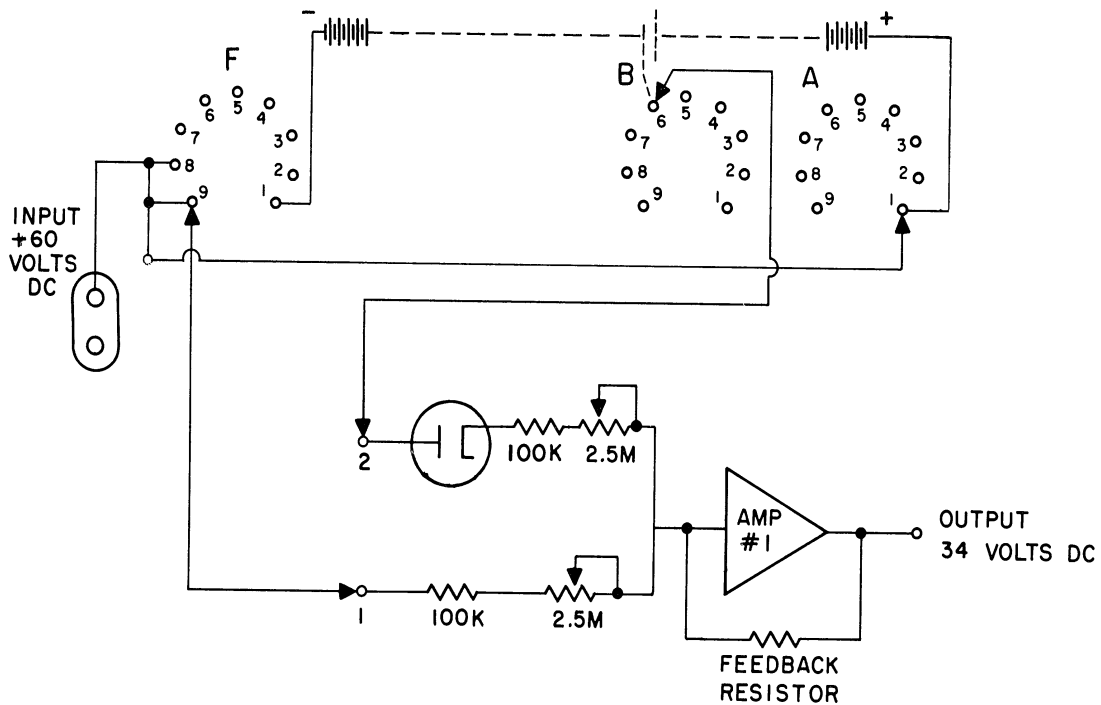
this function.) Since the dynamic range of the amplifiers in SIMRAR is 60 volts, it is desirable to scale the desired function to make most use of this range. Hence functions are usually set up for 60 volts output with 60 volts input. In Fig. 40, 4 segments are indicated, one starting at zero input. For the 3 other segments, the diodes are biased at the input voltages corresponding to the break points, 1, 2, 3,. These voltages must be integral multiples of $3/2$, since this is the incremental voltage in the battery supply. From the curve, the voltages are 21, 40.5 and 51 volts.

Figures 41 and 42 will help to explain how the function generator is set up for this function. For the first segment, the function generator input is connected directly to amplifier 1 input (no diode). This is the external connection from the amplifier input terminal marked "1" to pin F9, as shown in Fig. 41. This is also illustrated in Fig. 42. The function is set up segment by segment, with some known voltage input. An input of +60 volts is convenient, since it can be used for setup over the entire input range. Thus in Fig. 40, with 60 volts input, the output with the first segment only should be 23.5 volts. The 2.5 Megohm pot in the first input arm is therefore adjusted so that the output of the amplifier 1 is 23.5 volts. (The output voltage will be negative.)

For the second segment, the diode bias should be 21 volts. The diode plate is connected to the pickoff which gives this voltage, pin B6, as shown in Fig. 41. Now, with the first segment already properly set up, the output with both segments should be 34 volts at 60 volts input. So, the 2.5-megohm pot in the second input arm is adjusted to give 34 volts at the amplifier output. The procedure is continued for



(a) Setup for first segment.



(b) Setup for two segments.

Fig. 41. Function generator setup diagram.

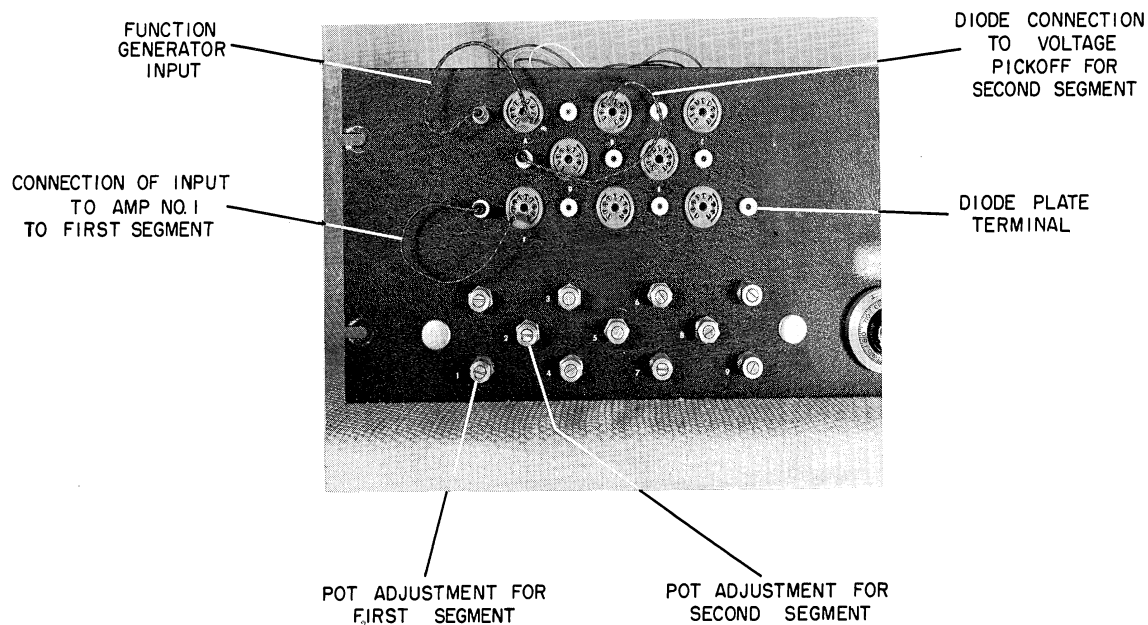


Fig. 42. Function generator setup, front view.

the other segments, first connecting the diode plate to the proper pickoff, and adjusting the corresponding pot to give the required output at 60 volts input. The pickoff voltages increase in the counter-clockwise direction on the A, B, C, etc., sockets with an increment of 1.5 volts between pins. The lowest voltage, 1.5 volts, is on pin A2. Pin A9 has 12 volts, pin B1 has 13.5 volts, pin B9 has 25.5 volts, etc.

On the function generator front panel, Fig. 42, the diode plate terminals are arranged in the same pattern as the potentiometers, with the pot which is in the same amplifier input branch occupying the corresponding position in the pattern.

The slope of any line segment in the function simulation is the total input-output gain of amplifier 1. This varies directly with

the feedback resistance for the amplifier, and with the sum of the reciprocal resistances in the input branches. The feedback resistance should be chosen sufficiently large to realize the largest slope required, considering that the minimum equivalent input resistance can be as large as 100K. It may occur, however, that with this feedback resistance the smallest slope required cannot be realized with the maximum input resistance, 2.6 megohms. In that case, external resistors may be inserted between the diode plate and the bias voltage pickoff. Some resistors are kept on the equipment for this purpose, and these were pointed out on Fig. 38. If the range of variation of slope is rather large, an accurate simulation may be difficult because of the large external resistances necessary to achieve small slopes. For example, if the largest slope is 20, a feedback resistor of 2 megohms would be necessary; but achieving a slope of .05 with this feedback resistor would require an external input resistor of 37.4 megohms.

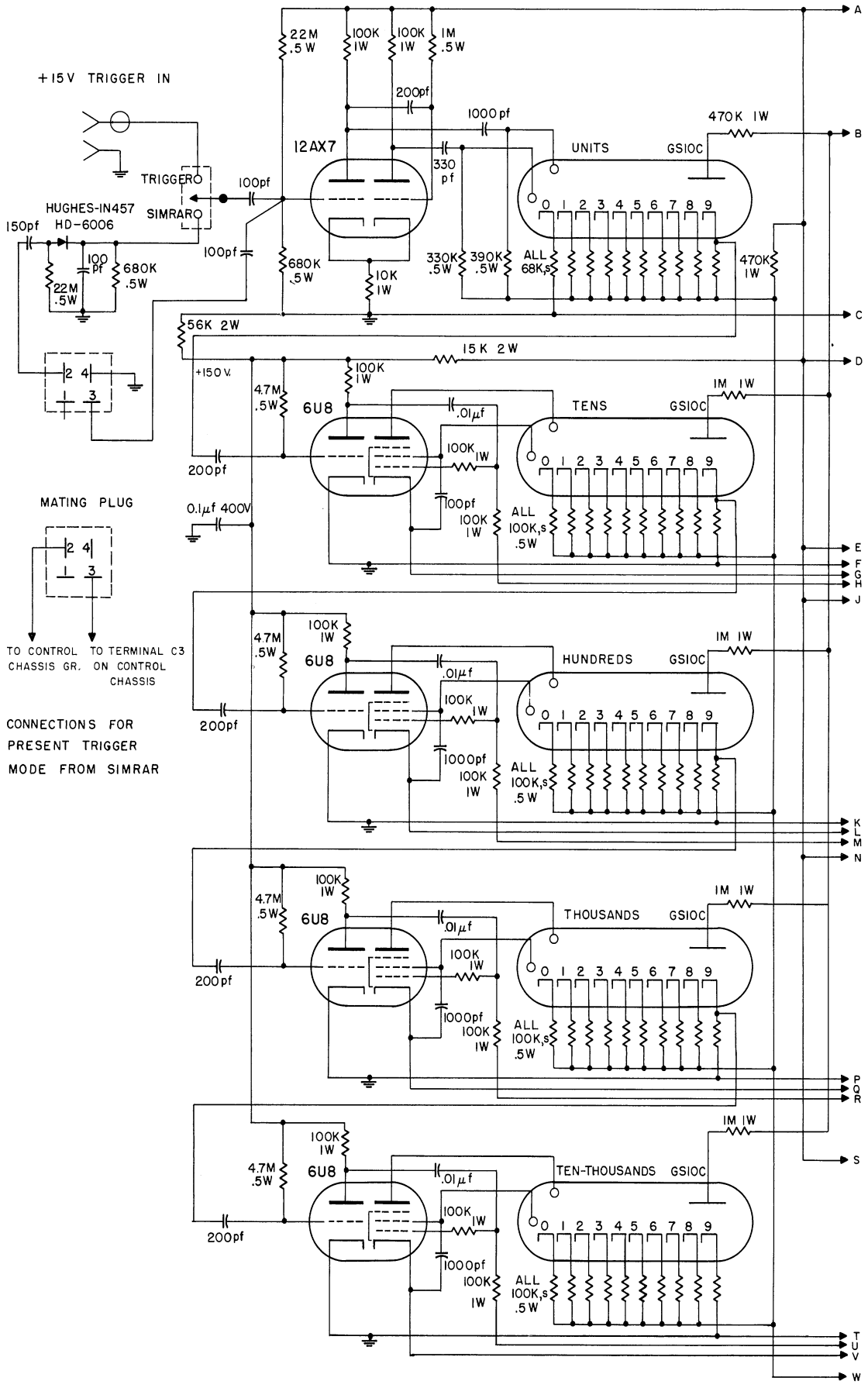
4.3.3 Voltage Divider. The voltage divider on the tuned amplifier-detector chassis is used as a known dc voltage source for experiments and setting up a simulation. Figure 43 is the schematic diagram. Figure 32 points out the various switches on the panel.

There are five voltage ranges available. Either polarity may be selected, and the voltage is continuously variable in the range. In order to obtain the designated voltage ranges, the voltage divider should be used with only one switch on.

The voltage divider output is available at the rear of the tuned amplifier-detector chassis. It is also fused on this chassis.

4.4 Preset Counter

The preset counter is used to stop the control circuit cycling of SIMRAR after a preset number of total trials has been accomplished.



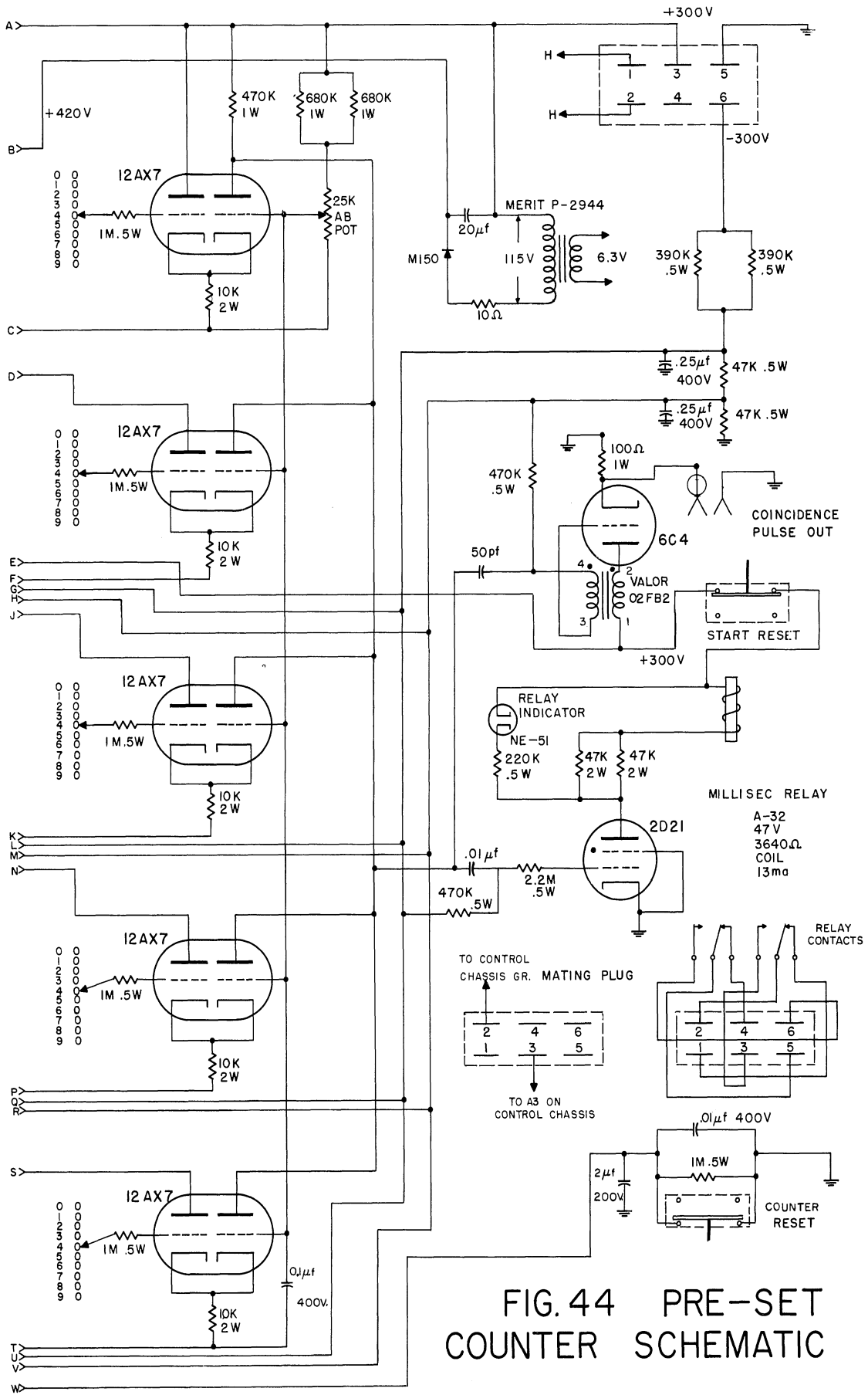


FIG. 44 PRE-SET
COUNTER SCHEMATIC

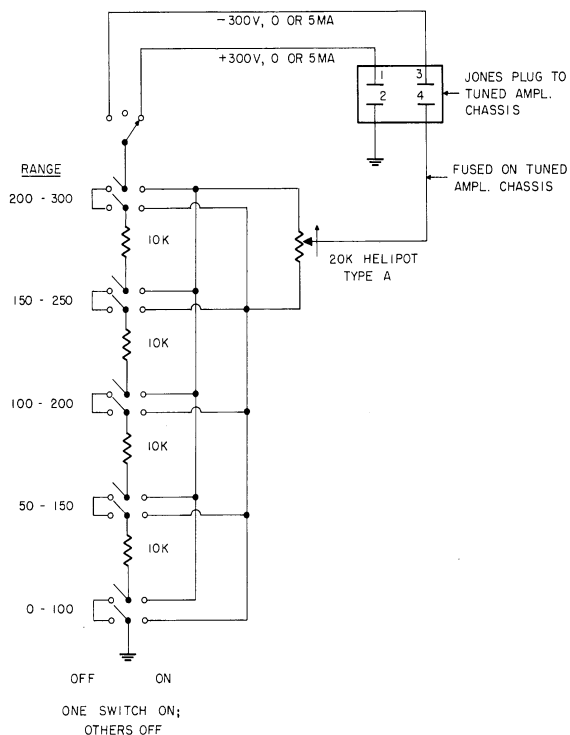


Fig. 43. Voltage divider schematic.

Relay contacts in the preset counter circuit effectively parallel the push-to-stop switch in the control circuit of SIMRAR. When the number of trials has been completed, a coincidence circuit operates the relay, producing the same effect as operation of the push-to-stop switch.

The circuit uses 5 Atomic Instrument Company GS10C glow transfer counter tubes, permitting a total count of 99,999 trials. The circuit may be triggered from three sources: an external trigger pulse of +15 volts peak, a +125 volt

trigger pulse from SIMRAR, or a pulse obtained from the 6AQ5 grid in the control circuit of SIMRAR. The latter is the present mode of operation with SIMRAR.

Figure 44 is the schematic diagram of the circuit. Figures 45 and 46 illustrate prominent features of the equipment. The trigger pulse from the 6AQ5 grid in SIMRAR occurs when the HG I relay opens at completion of a detection trial. This grounds the 6AQ5 grid which has been previously at about -45 volts. A positive pulse thereby appears at the left grid of the 12AX7 in the preset counter trigger input circuit. The 12AX7 is a triggered multivibrator, with the left half normally cut off. Arrival of the pulse from SIMRAR changes the state of the circuit, producing a negative pulse at pin 12 of

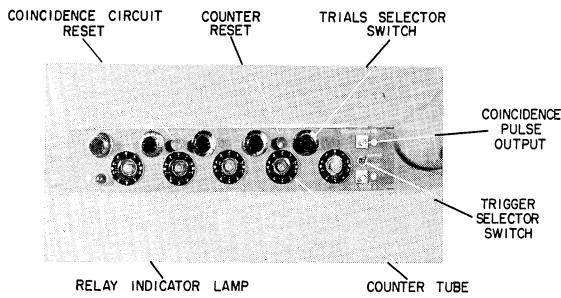


Fig. 45. Preset counter, front view.

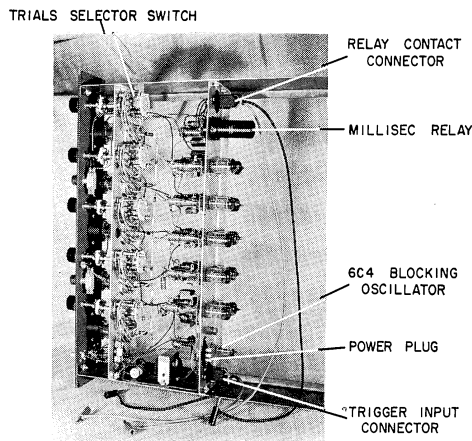


Fig. 46. Preset counter, back view.

the first GS10C, and a positive pulse at pin 11. These two tube elements (guides 1 and 2, respectively) control the glow transfer between the anode and the 10 cathodes. When the glow moves to a cathode, the cathode swings positive from ground to about 25 volts.

The cathode corresponding to a count of 9 on the units counter is coupled through a 6U8 driving circuit to the tens counter. Because of the normal state of the driving circuit, no action takes place when the glow transfers

to the #9 cathode of the units counter. When the glow leaves, however, a negative pulse occurs at the 6U8 triode grid of the tens counter driving circuit. The driving circuit produces a negative pulse at guide 1 (pin 12) of the tens GS10C counter tube, which results in glow transfer. The following counter tubes are driven in identical manner from the preceding counter stage. A running count is thereby made of the trials completed, the count being determined by the position of the glow on the radially-spaced cathode around the central anode of each counter tube. The maximum input frequency for the counter tubes is 4000 pulses/sec.

The coincidence circuit for the present counter consists

of five 12AX7 stages in parallel, each stage operating in conjunction with one counter stage. The selector switches, through which the total trials-to-be-counted is selected, connect the left grid of each 12AX7 stage to the appropriate cathode of the corresponding counter tube. For example, if 1000 trials are to be made, selection of this number on the switches connects the first three 12AX7 stages to the 0 cathode of the units, tens, and hundreds counters, respectively. The fourth 12AX7 stage is connected to the No. 1 cathode of the thousands counter. The 12AX7's are connected in parallel in the sense that the right halves have a common plate-load resistance, 470K, from the +300 volt supply, and a common bias obtained from a voltage divider on the +300 volt line. The value of this bias is critical in the operation of the coincidence circuit.

As stated previously, a cathode of a counter tube will swing positive when the glow is on that cathode. Then, when the total number of trials selected has been completed, the left grid of every 12AX7 stage in the coincidence circuit will be positive, and the left halves in fairly heavy conduction. The bias produced by this conduction through the common cathode resistor will be sufficient to cut off, or nearly so, the right half of each 12AX7. The right plates, which are capacitively coupled to the grid of a 2D21 thyratron, will rise to nearly +300 volts, firing the thyratron. Conduction through the thyratron energizes the A32 Millisec relay, which closes, connecting the push-to-stop contact, A3 on the control chassis terminal board, to ground. Since operation of the relay produces effectively the same result as manual operation of the push-to-stop switch, cycling of the control circuit of SIMRAR ceases.

The bias of the 12AX7 stages must be adjusted so that with the right half of one in conduction (the glow of the corresponding counter tube is not on the cathode connected to the left grid), and the others in parallel suddenly cut off, the voltage rise at the plate is not sufficient to fire the thyatron. That is, the bias is adjusted so that the thyatron fires if and only if all the right halves are cut off at once. Then the coincidence circuit operates to stop SIMRAR only when every counter is in the condition corresponding to completion of the preset number of total trials.

The counter reset push-button resets all counter tubes to zero. The start reset push-button, by removing the +300-volt supply from the thyatron, de-energizes the Millisec relay and hence resets the coincidence circuit for another run. The relay indicator lamp provides a visual indication of the relay condition.

A coincidence pulse is generated for external use in the 6C4 blocking oscillator, which is triggered by operation of the coincidence circuit of the preset counter. This pulse has an amplitude of about +20 volts, and duration of several microseconds.

4.5 Power Supply

The power supply of SIMRAR provides +300 and -300 volts dc, +125 volts dc for recording, and 6.3 volts ac for tube filaments. Figure 47 is a schematic diagram of the power supply. Figures 48 and 49 are front and rear views.

AC power is brought to the SIMRAR rack from the external line, and made available on terminals on the right side of the rack. A switch at the bottom of the rack controls the ac power, and a meter is provided for monitoring the ac line voltage. AC power is brought to the SIMRAR

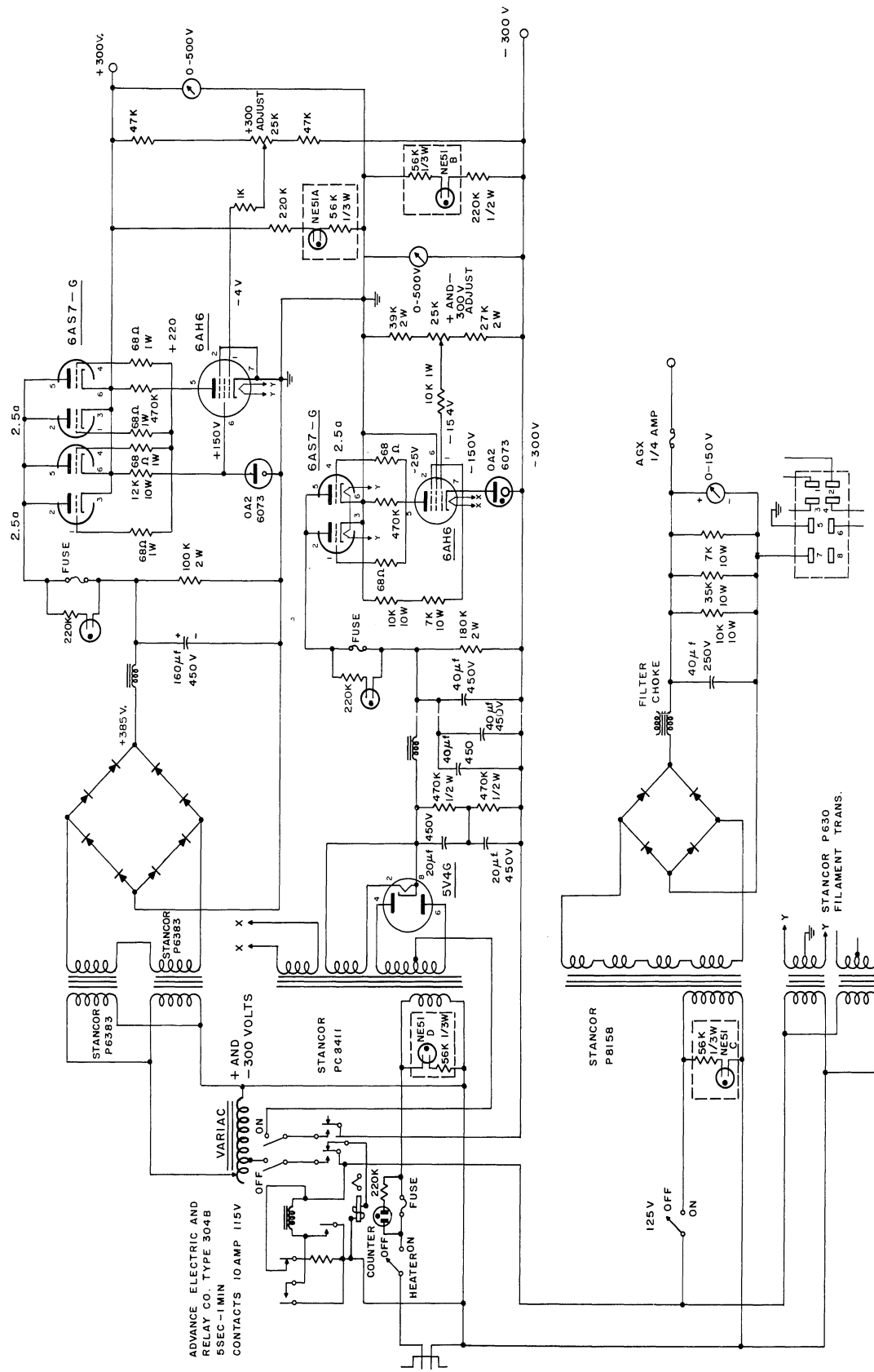


Fig. 47. Power supply schematic diagram.

power supply from the rack terminals. Upon operation of the "Heaters" switch, the line voltage is connected to the filament transformer primaries. The line voltage is not connected to the power transformers until a time delay, determined by the relay, has elapsed. This prevents connection of high voltage to equipment before the high voltage regulator circuits are sufficiently warmed up to provide good regulation.

The "+ and -300" switch, in conjunction with the time delay relay, controls the connection of ac line voltage to the power transformers of the + and -300-volt dc supplies. The +300-volt supply uses selenium rectifiers in a bridge circuit to achieve full-wave rectification, while the -300-volt supply utilizes a 5V4G full-wave rectifier. Both supplies have similar vacuum tube voltage regulating circuits, consisting of 6AS7-G regulator tubes controlled by a 6AH6 pentode, with a 6073 (0A2) as the voltage reference tube. Two 6AS7-G tubes are used in the +300-volt supply to provide a greater current capability. The supply voltages have a common adjustment, with a separate adjustment provided for the +300-volt supply. Meters are provided to monitor the supply voltages. Indicator lamps and fuses are included in the circuit.

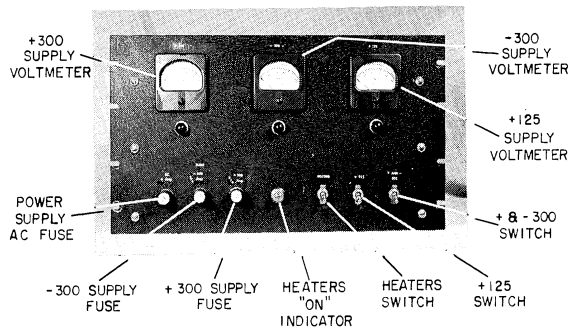


Fig. 48. Power supply, front view.

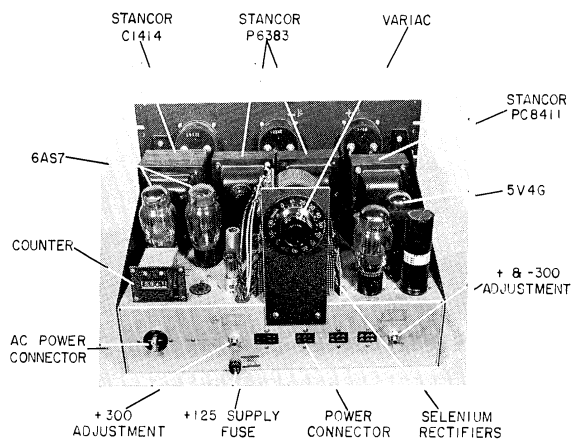


Fig. 49. Power supply, rear view.

The +125 volt power supply uses selenium rectifiers in a bridge circuit. AC power to the transformer is controlled by the "+125 volts" switch. This power supply is not regulated, since it is used to supply SIMRAR circuits where requirements on power stability are not critical. A voltmeter is included to monitor the supply voltage.

Table III gives the approximate measured current requirements on the several power supplies in SIMRAR. Table IV gives the measured currents to the various chassis in SIMRAR for the high voltage supplies.

TABLE III.

MEASURED POWER SUPPLY CURRENTS			
Supply Volts	+300	-300	+125
Total Current Stopped (ma.)	215	78	20
Total Current Running at 8 Trials/sec. (ma)	205	78	70*/28**

* noise input to discriminators
 ** no input to discriminators

TABLE IV.

BREAKDOWN OF HIGH VOLTAGE SUPPLY CURRENTS

Supply Volts	+300	-300
Control Chassis	45 ma	27 ma
Counter Chassis	95	11
Simulator Chassis	39	38
Preset Counter	25	1

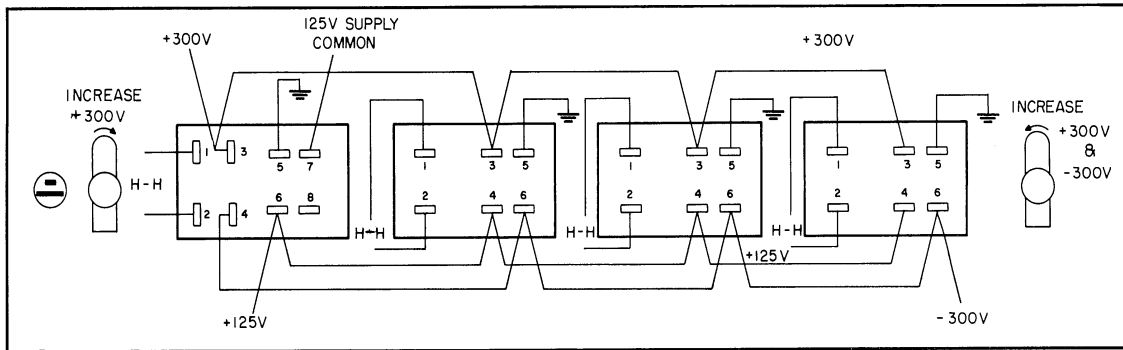


Fig. 50. Power supply plug connections.

4.6 Miscellaneous Equipment

4.6.1 Noise Source. The noise source in SIMRAR is a General Radio Type 1390A noise generator, Serial No. 509. The rms noise voltage output is continuously variable to as high as 5 volts rms output. The bandwidth of the noise output can be selected as 20 kc, 500 kc, or 5 msec.

For detailed information on this instrument, the reader is referred to the manufacturer's literature.

4.6.2 Delayed Pulse Generator. The delayed pulse generator circuit, Fig. 51, is to be used with the 10-kc tuned amplifier in SIMRAR,

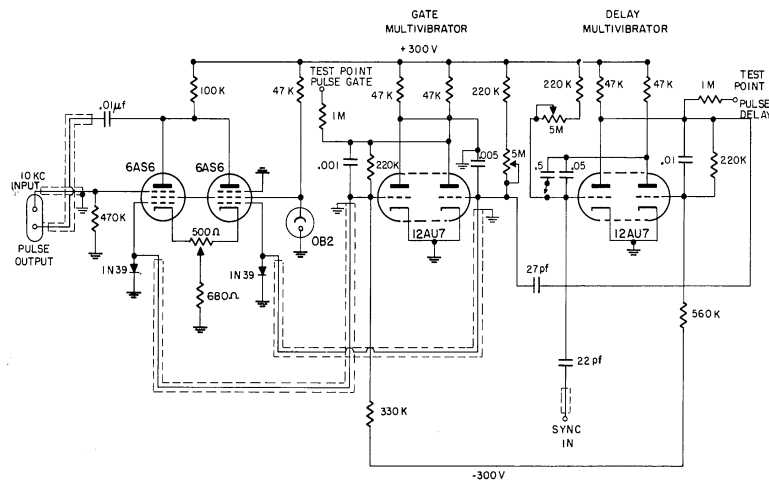


Fig. 51. Delayed pulse generator schematic.

for studies involving pulse signals. The circuit provides a sine wave pulse, of variable duration, with an adjustable starting time after a sync pulse. Inputs to the circuit are the sync pulse, and a continuous 10-kc sinusoidal signal.

Two monostable multivibrator circuits are used. The "delay multivibrator" provides delay between the occurrence of the sync pulse and the starting time of the pulse output of the circuit. The "gate multivibrator" provides a pulse of proper duration which is used to gate the continuous 10-kc input, and thereby generate the pulse output.

The sync pulse for the circuit can be obtained from the 6AQ5 plate in the control circuit. This waveform rises exponentially toward +300 volts during the off time of SIMRAR and drops abruptly to about 50 volts when a detection trial begins (opening of HG I relay). Then at the left grid of the delay multivibrator, a large negative pulse will appear at the beginning of a detection trial. The stable state of the delay multivibrator is the left half conducting, right half cut off. The sync pulse switches the circuit into the unstable state. After a delay determined by the time constant of the left grid circuit, the tube switches back to the stable state. This delay is the time between the occurrence of the sync pulse and the starting time of the pulse output of the generator. It can be varied by changing the grid circuit time constant, either with the pot adjustment or switching the capacitor.

At each switching of the delay multivibrator, a voltage step occurs at the left plate, which is coupled through a 27pf capacitor to the right grid of the gate multivibrator. The first step produces

a positive pulse at the gate multivibrator grid, while the next produces a negative pulse. The gate multivibrator stable state is the right half conducting, left half cutoff. The positive pulse from the delay multivibrator doesn't disturb the circuit. The negative pulse, however, switches the circuit into the unstable state. The tube switches back to the stable state after a delay determined by the time constant of the right grid circuit. This delay is the width of the output pulse of the generator, and is adjustable through the 5-megohm potentiometer.

The 6AS6 pentode operates in parallel with the gate multivibrator. Corresponding to the stable state of the gate multivibrator, the right half of the 6AS6 is normally conducting with the left half cutoff. The 10-kc input on the suppressor grid of the left half does not appear at the output. With the gate multivibrator in the unstable state, the right half of the 6AS6 is cut off, and the 10-kc signal is gated through the left half. When the gate multivibrator returns to the stable state, the 10-kc output is shut off.

The output pulse duration is adjustable about the value of the time constant of the impulse response of the 10-kc tuned amplifier in SIMRAR. The delay of the pulse can be adjusted to place the pulse position anywhere in the observation interval of SIMRAR.

Figures 52 to 54 illustrate the waveforms in the pulse generator circuit. By adding a larger capacitor in the right grid circuit of the gate multivibrator, the circuit could also be used to generate pulses for the 1-kc tuned amplifier of SIMRAR. Figure 55 is a back view of the delayed pulse generator.

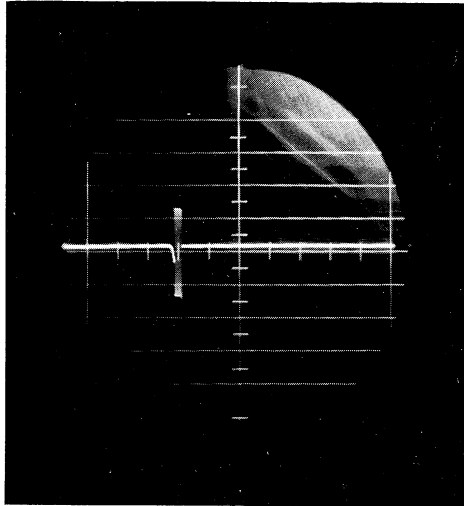


Fig. 52. 10 kc/s pulse output of delayed pulse generator.
20 v/cm vertical
10 ms/cm horizontal

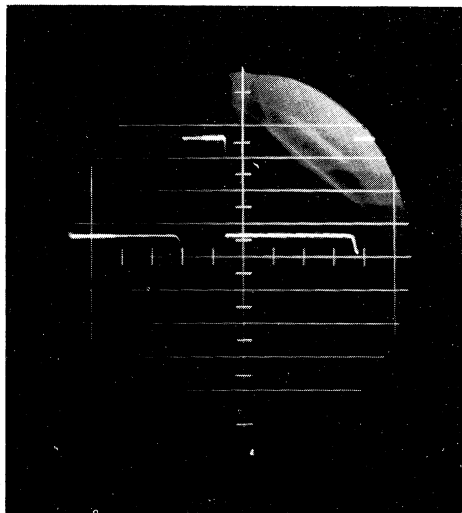


Fig. 53. Delayed pulse generator--pulse delay test point waveform
60 v/cm vertical
10 ms/cm horizontal

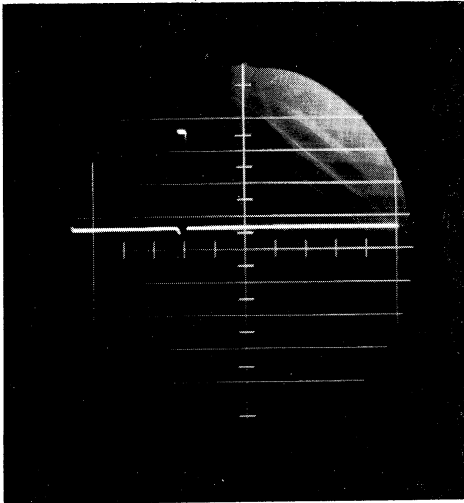


Fig. 54. Delayed pulse generator-pulse gate test point wave.

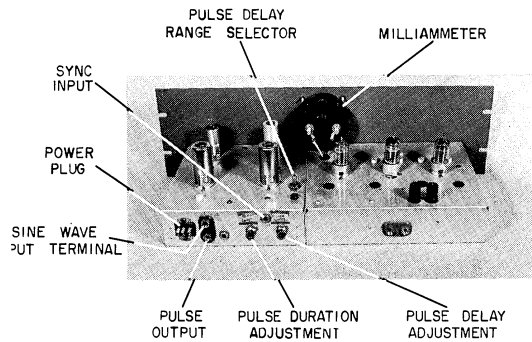


Fig. 55. Delayed pulse generator, back view.

4.6.3 Squaring Circuit. The squaring circuit, Fig. 56, provides a measured output current which is proportional to the square of the input voltage. The first stage is a differential amplifier, having push-pull outputs, driving the next stage. The plate current of each half of the second stage can be closely approximated in the operating region by a power series expansion in terms of the grid voltage, of degree two. Since this stage is driven push-pull, all terms of odd degree will cancel, and the total plate current will be proportional to the square of the grid voltage with an additional constant value. The symmetrical last stage balances out the constant value of plate voltage, so that the milliammeter measures a current which is proportional to the square of the input voltage.

The adjustment procedure is as follows:

(1) With zero input, adjust the input balance so that the voltages at test points 1 and 2 are equal.

(2) Set the bias adjustment so that the voltages at test points 1 and 2 are approximately -10 volts.

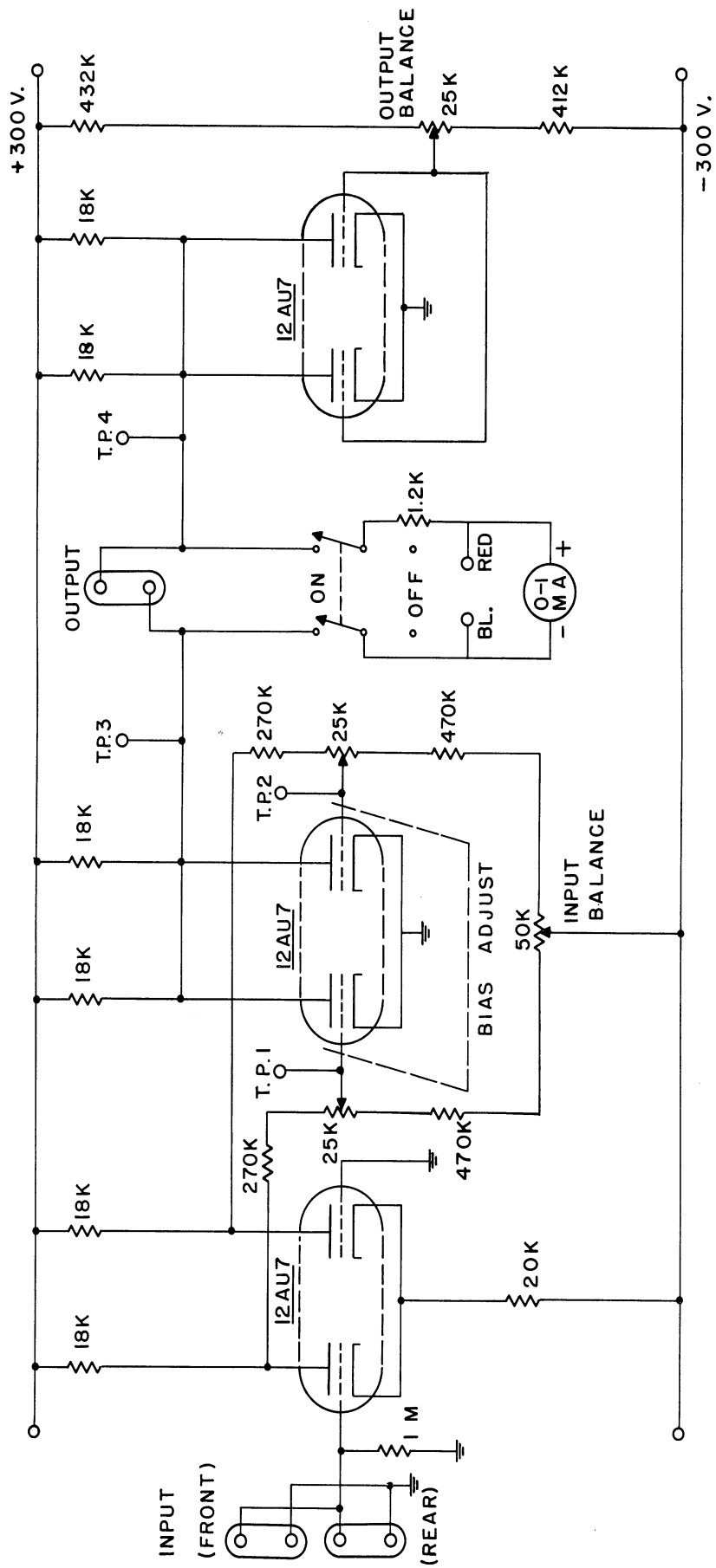


Fig. 56. Schematic diagram of squaring circuit.

(3) Set the output balance so that the meter reads zero.

(The meter may be disconnected, using the switch, for the preceding two steps).

(4) With a sine wave input (up to 400 cps), make a fine adjustment of the input balance to give a pure second harmonic from test point 3 to ground. The Lissajous pattern on an oscilloscope is convenient for this adjustment.

The milliammeter can be calibrated with a dc input to give a voltage reading of the input squared. This circuit has application in a measurement circuit to give the true mean squared value of an arbitrary input waveform.

5. DETAILED DESCRIPTION OF A TYPICAL SIMULATION

A detailed description of a typical signal detection problem which can be studied with SIMRAR is given here, in order to explain more fully the experimental procedure and how the operational features of each equipment are utilized in a simulation.

Consider the problem of detecting with a broadband receiver a constant amplitude signal, known completely except for uniformly distributed phase. Reference 1 discusses the optimum video design for this case. The receiver consists of a bandpass filter, linear detector, and an integrator, for large signal-to-noise ratio. The decision is made at the end of the observation interval, which in the present discussion is the duration of the signal. Figure 57 illustrates the complete simulation for this problem.

Since this is a fixed time duration situation, the negative timing wave is used as input to the No. 11 discriminator, and the No. 11 discriminator is used as termination supply for the control circuit.

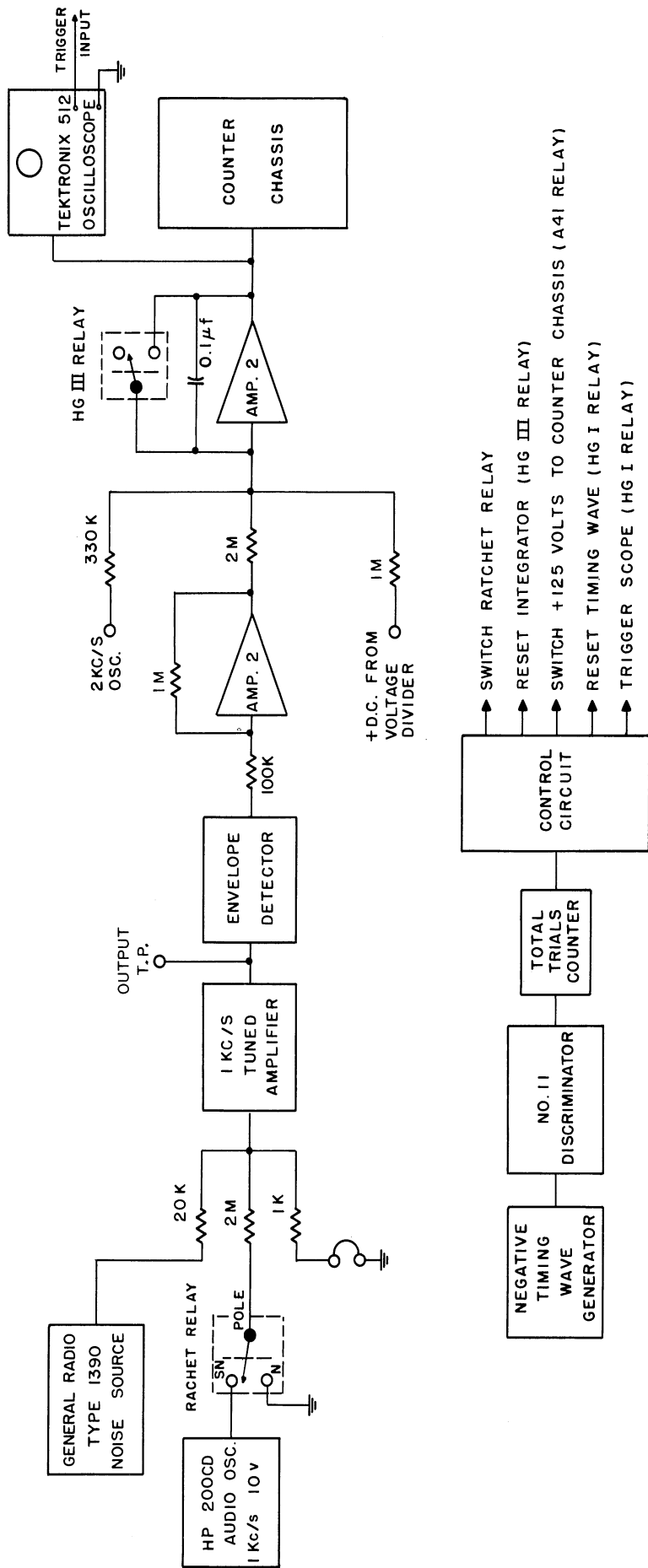


Fig. 57. Simulation for broadband reception of constant amplitude signal completely known except for phase.

The signal duration (observation time) was chosen as 59 milliseconds. Since the impulse response time of the 1-kc tuned filter in SIMRAR is about 15 milliseconds, this corresponds to the broadband reception case. (The ideal receiver has an impulse-response time constant which is approximately equal to the duration of the signal. The impulse-response time constant of a simple tuned filter is the reciprocal of the total bandwidth. Since here the impulse-response time is shorter than the signal duration, it indicates that the bandwidth of this receiver is broader than that of the ideal receiver.) The duration is conveniently adjusted by observing the "external trigger" pulse output of the Tektronix oscilloscope, with the trigger output gated through the HG I relay of SIMRAR. The sweep duration can be set to the desired observation time, and the observation interval range switch and threshold level for the No. 11 discriminator can be adjusted to obtain the desired interval.

The signal-to-noise ratio at the output of the tuned filter can be varied by changing either the input signal amplitude or the noise level. The signal-to-noise ratio ($\frac{S}{N}$) is found by individually measuring with a Ballantine 320 True RMS Voltmeter the rms noise and continuous signal amplitude at the filter output test point. If these values are V_N and V_S ,

$$\frac{S}{N} = \left(\frac{V_S}{V_N} \right)^2 \quad (2)$$

A constant amplitude signal of 10 volts rms was used at the simulation input, which gave a signal amplitude of 14 volts at the filter output. Figure 58 is a plot of the noise generator rms volts output (as measured by the meter on the front panel of the General Radio noise source)

against the rms noise voltage at the tuned filter output for this simulation. Then, for example, if the noise generator output is adjusted to 4 volts rms, with the 10-volt rms signal input, the signal-to-noise ratio at the filter output is

$$\frac{S}{N} = \left(\frac{14}{17.4}\right)^2 = 0.65 \quad (3)$$

The small dc voltage added at the integrator reduces the mean value of the amplifier No. 2 output, and permits use of higher gain in the integrator. More effective use of the range of the discriminators can thereby be obtained. The gain of amplifier No. 2 and the integrator gain are not critical in this problem representation, but are selected to give a reasonable range of output amplitude consistent with the range of the amplifiers and discriminators. Having scaled the problem in this respect, the threshold levels of the discriminators can be chosen according to the expected distribution of the output amplitudes. Usually, in a signal detection study, one will not be concerned with the voltage level of the thresholds, but will attempt to achieve a range of false alarm probabilities for which the detection probabilities are conveniently measurable (less than 0.99). As pointed out in Section 3.3, this range will be restricted by accuracy limits if the detection performance is very good,

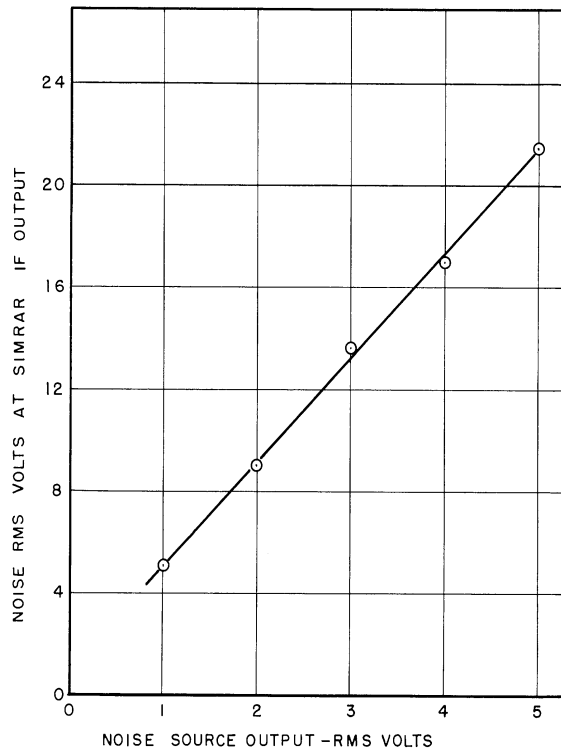


Fig. 58. SIMRAR noise calibration curve.

but a range from 0.05 to 0.85 is generally satisfactory. A short run of 100 trials on each alternative will help to determine that the threshold settings will give reasonable data.

A run of 1000 trials per alternative (2000 total trials) will give good statistical accuracy in the data. Table V presents the probability estimates obtained from 2000 total trials in the simulation of Fig. 57. The values are obtained by dividing the counter readings by 1000, the number of trials of each alternative. Figure 59 is a plot of the probability estimates on normal-normal probability paper. This plot is known as the "receiver operating curve" (Ref. 1), from which a single measure of detection performance, the parameter d' , can be obtained (Ref. 2).

Figures 60 through 64 illustrate some typical waveforms in this simulation. In the next section, data obtained from this simulation will be used to describe the performance of SIMRAR in statistical measurements.

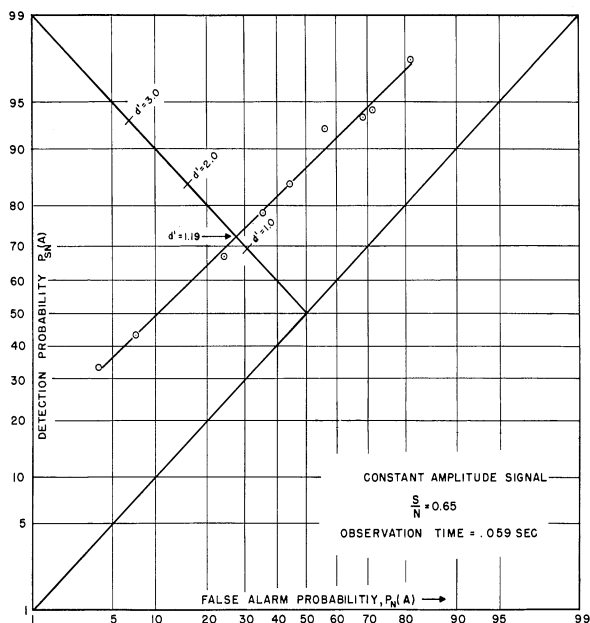


Fig. 59. Receiver operating curve of broadband receiver.

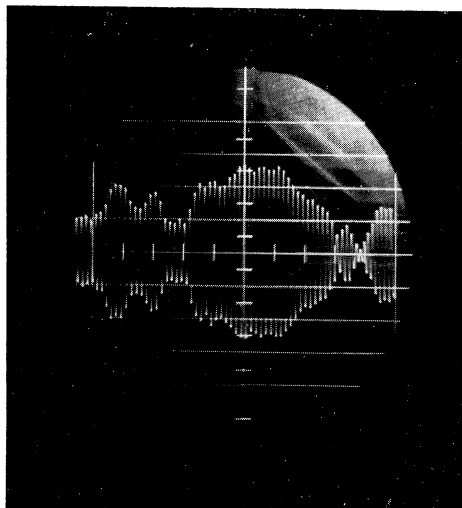


Fig. 60. Tuned amplifier output, signal and noise present.

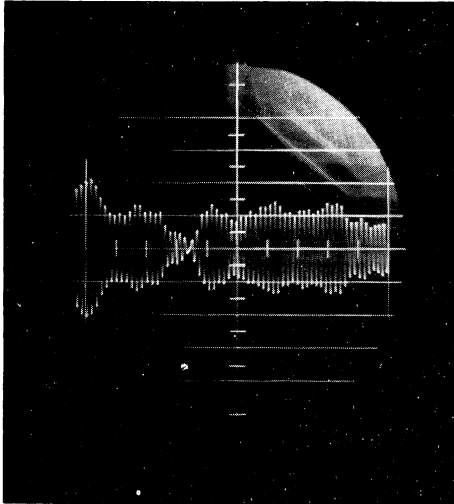


Fig. 61. 1 kc/s tuned amplifier
output: noise alone present.
20 v/cm vertical
5.9 ms/cm horizontal

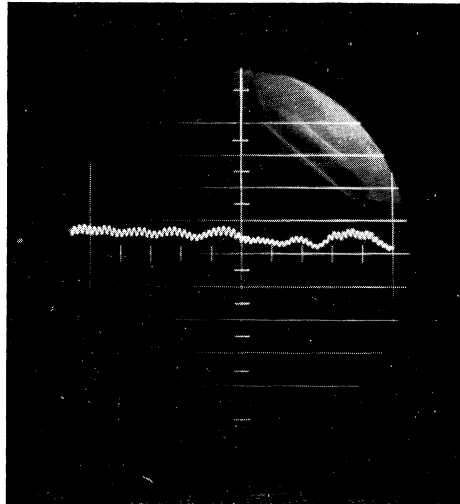


Fig. 62. Detector output: signal
and noise present.
20 v/cm vertical
5.9 ms/cm horizontal

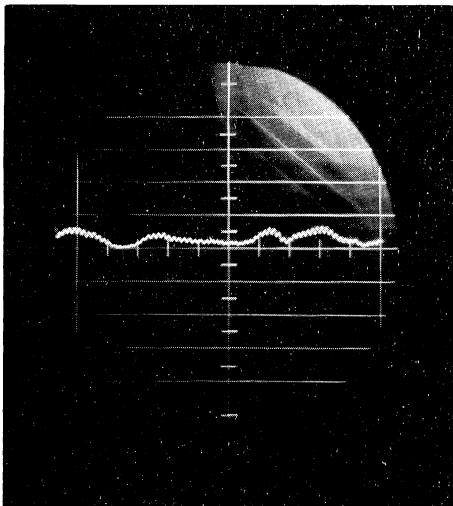


Fig. 63. Detector output: noise
alone present.
20 v/cm vertical
5.9 ms/cm horizontal

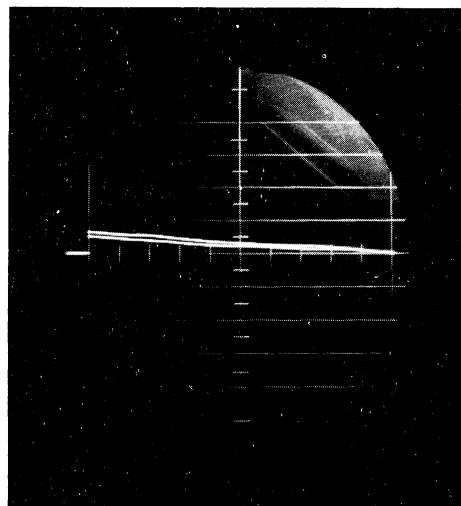


Fig. 64. Integrator output: SN and
N waveforms on two consecutive
trials.
20 v/cm vertical
5.9 ms/cm horizontal

TABLE V.

PROBABILITY ESTIMATES FOR

$$\frac{S}{N} = 0.65, 2000 \text{ TOTAL TRIALS}$$

Discrim. No.	#1	#2	#3	#4	#5	#6	#7	#8	#9
Threshold Pot Setting	125	130	135	150	160	170	190	210	220
$P_{SN}(A)$.976	.942	.937	.925	.842	.782	.672	.432	.336
$P_N(A)$.813	.715	.688	.564	.447	.357	.243	.073	.039

6. PERFORMANCE OF SIMRAR IN STATISTICAL MEASUREMENTS

In SIMRAR, the question of accuracy of measurements is overshadowed by the problems of drift and stability. Accuracy is limited by how well the simulation realizes the actual problem, the total number of trials taken, and the accuracy of test equipment (voltmeters, for example) which may be used to set threshold levels, measure signal amplitudes, and adjust observation time, etc. However, because periods of time as long as half an hour may be required to obtain a single set of data, the normal drift in amplifier dc output and gain, fluctuations in the power supply, signal sources, timing circuits, and other equipment may result in larger discrepancies in the measured data than initial inaccuracies in setting up the equipment.

As an example of the dc drift to be expected in the amplifiers of SIMRAR, Fig. 65 is a short time recording of the output of the tuned amplifier-detector, and a cascade of the tuned amplifier-detector, amplifier 2, and amplifier 3. The input grid of the tuned amplifier was grounded, with amplifier 2 acting as a unity gain amplifier, and

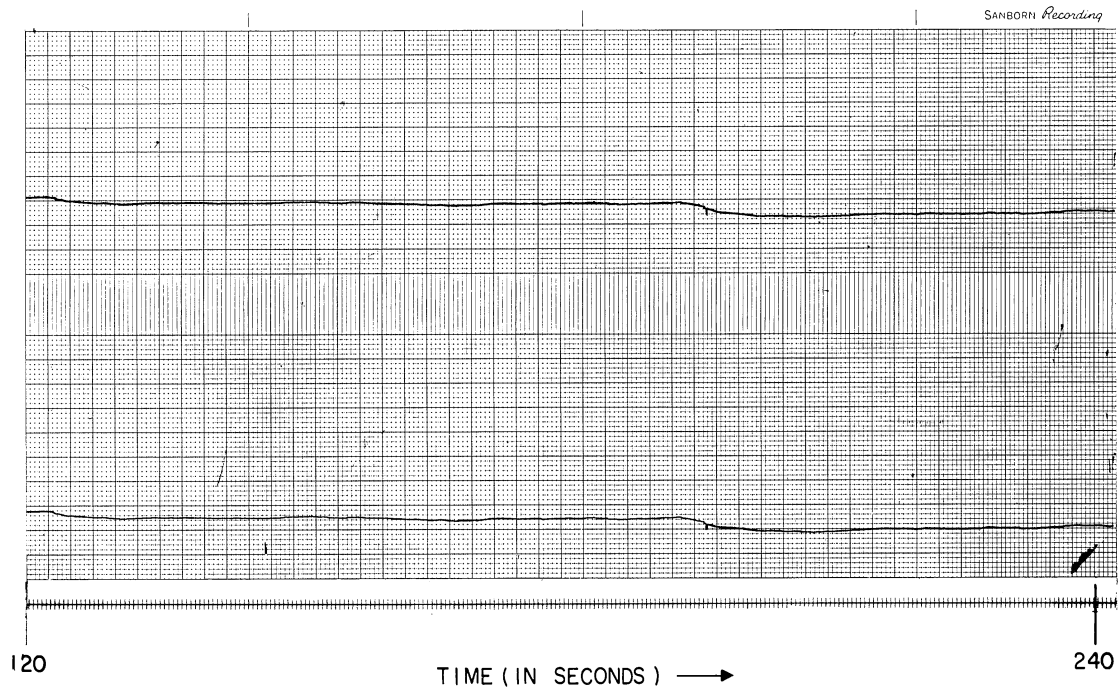
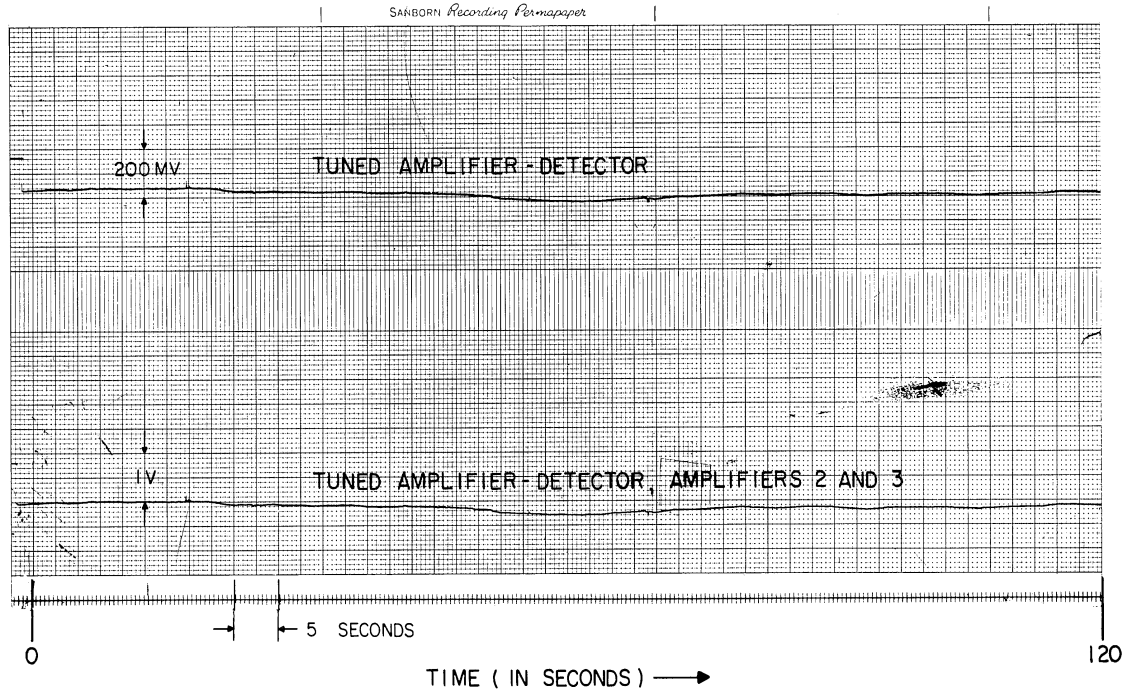


Fig. 65. SIMRAR amplifier dc drift after 25-minute warmup.

amplifier 3 set up as a low-pass filter amplifier of 40 cps bandwidth and gain of 6. No attempt was made to initially balance the amplifiers, although it should be noted that the initial balance of the tuned amplifier is about as good as can be obtained. Over a period of 5 minutes, the dc output varies from the initial value by as much as 50 mv for the tuned amplifier only, and 0.2 v for the cascade of the three amplifiers. One can also see that the fluctuations in output of the cascade follow closely the fluctuations of the tuned amplifier output. This would be expected because the tuned amplifier-detector has the largest drift of the amplifiers in the simulator. Over periods of several hours, its average dc drift would be about 90 mv/hour. The drift of amplifiers 2 and 3 is small in comparison.

The SIMRAR sequence of alternation between receiver inputs of signal-and-noise and noise alone tends to minimize the effects of drifts on the data obtained in signal detection studies. The important quantity here is the parameter d' , the difference in the means of normal distributions with signal-and-noise, and noise alone, which can be used as a single measure of detection performance. As SIMRAR consecutively makes a detection trial on one alternative input, and then the other, the mean of each distribution may drift, but only very short time fluctuations which occur more consistently on one alternative than the other will affect the difference in the means. Hence, the difference in the means will remain relatively constant.

An illustration of the effect of drift is the result of repeated measurements of the same distribution over a long period of time. Here the question of the statistical inaccuracy of the data, as a re-

sult of taking only a finite number of trials, must be resolved. Using the simulation of the previous section, repeated measurements were obtained over one day of the distributions with signal-and-noise, and noise alone. On each run, 2000 total trials (1000 per alternative) were taken. The 1-kc signal amplitude and the noise power were adjusted to the initial values ($\frac{S}{N}$ at the IF filter = 0.65) before each run, but no attempt was made to maintain the setting of other quantities.

Tables VI, VII, and VIII present an analysis of the data. The mean measured probability is the average of the 10 probability estimates from each counter,

$$\bar{p} = \frac{1}{10} \sum_{i=1}^{10} p_i. \quad (4)$$

The standard deviation of the measured probability is the estimate of the standard deviation of the probabilities from each counter, based on the small sample of 10 runs,

$$\sigma = \left[\frac{10}{9} \left(\frac{1}{10} \sum_{i=1}^{10} p_i^2 - \bar{p}^2 \right) \right]^{\frac{1}{2}} \quad (5)$$

The binomial standard deviation of the mean probability, \bar{p} , is an indication of the statistical inaccuracy due to the number of trials taken. If the true probability is the mean probability, the statistical error in any one measurement of n trials has the binomial standard deviation.

$$\sigma_B = \sqrt{\frac{\bar{p}(1 - \bar{p})}{n}} \quad (6)$$

This was previously plotted in Fig. 5 for several values of n . Here, $n = 1000$. The ratio of the standard deviation of the measured probabilities

TABLE VI
DATA FOR SIGNAL-AND-NOISE DISTRIBUTION

Run	Time of Completion (Hrs:Min)	PROBABILITY ESTIMATES FROM COUNTERS								
		1	2	3	4	5	6	7	8	9
1	0:07	.992	.979	.977	.787	.663	.652	.340	.241	.177
2	0:16	.986	.974	.971	.779	.663	.655	.321	.223	.160
3	0:27	.984	.961	.959	.757	.633	.618	.326	.218	.167
4	1:00	.985	.964	.963	.747	.633	.617	.320	.219	.163
5	1:47	.986	.973	.969	.778	.656	.638	.326	.204	.145
6	2:17	.979	.962	.957	.755	.619	.607	.319	.198	.132
7	4:56	.993	.970	.968	.778	.643	.622	.321	.214	.156
8	5:05	.988	.972	.968	.777	.667	.656	.353	.216	.148
9	6:40	.986	.972	.969	.768	.629	.612	.297	.194	.130
10	7:20	.981	.961	.957	.772	.629	.609	.308	.203	.156
MEAN MEASURED PROBABILITY		.9860	.9688	.9658	.7698	.6435	.6286	.3231	.2130	.1534
STANDARD DEVIATION, σ , OF MEASURED PROBABILITY		4.31/1000	6.34/1000	6.599/1000	12.79/1000	17.31/1000	19.7/1000	15.4/1000	13.81/1000	14.9/1000
BINOMIAL STANDARD DEVIATION OF MEAN PROBABILITY		3.7/1000	5.5/1000	5.7/1000	13.2/1000	15.1/1000	15.2/1000	14.6/1000	13.0/1000	11.4/1000
RATIO OF STANDARD DEVIATIONS		1.163	1.17	1.158	0.97	1.147	1.297	1.055	1.062	1.308

TABLE VII
DATA FOR NOISE-ALONE DISTRIBUTION

Run	Time of Completion (Hrs:Min)	PROBABILITY ESTIMATES FROM COUNTERS								
		1	2	3	4	5	6	7	8	9
1	0:07	.950	.885	.878	.400	.263	.247	.056	.019	.005
2	0:16	.925	.840	.829	.273	.221	.203	.045	.016	.006
3	0:27	.918	.836	.826	.326	.201	.190	.036	.017	.006
4	1:00	.910	.844	.830	.348	.240	.233	.060	.021	.012
5	1:47	.910	.832	.824	.347	.219	.213	.058	.025	.007
6	2:17	.884	.800	.792	.310	.220	.207	.054	.025	.011
7	4:56	.918	.851	.845	.365	.227	.219	.055	.021	.009
8	5:05	.926	.842	.836	.367	.250	.238	.057	.027	.014
9	6:40	.936	.873	.869	.388	.260	.246	.072	.035	.019
10	7:20	.928	.848	.843	.360	.239	.277	.050	.020	.009
MEAN MEASURED PROBABILITY		.9205	.8451	.8372	.3484	.2340	.2223	.0543	.0226	.0098
STANDARD DEVIATION, σ , OF MEASURED PROBABILITY		17.52/1000	22.87/1000	24.1/1000	37.59/1000	19.75/1000	19.1/1000	9.46/1000	5.71/1000	4.34/1000
BINOMIAL STAN- DARD DEVIATION OF MEAN PROB- ABILITY		8.5/1000	11.3/1000	11.6/1000	15.0/1000	13.2/1000	13.1/1000	7.1/1000	4.65/1000	3.10/1000
RATIO OF STANDARD DEVIATIONS		2.061	2.025	2.08	2.506	1.495	1.458	1.333	1.228	1.40

TABLE VIII

d' VALUES

Run	Time of Completion (Hrs:Min.)	d'	Mean d'	Standard Deviation of d' Values	Binomial Standard Deviation of Mean d'	Ratio of Standard Deviation
1	0:07	1.06	1.059	.0633	.0587	1.078
2	0:16	1.16				
3	0:27	1.09				
4	1:00	1.02				
5	1:47	1.13				
6	2:17	1.06				
7	4:56	1.07				
8	5:05	1.07				
9	6:40	.95				
10	7:20	.98				

σ , to the binomial standard deviation of the mean probability σ_B , is an indication of the additional deviation introduced by drifts in the machine. This ratio is given in the tables for the counter readings, and the d' values.

If one considers that the total variance in the measured data is the sum of the variance due to statistical inaccuracy, given by the binomial variance, and a variance resulting from machine drifts,

$$\sigma_{TOTAL}^2 = \sigma_B^2 + \sigma_{MACHINE}^2 \quad (7)$$

then

$$\frac{\sigma_{MACHINE}^2}{\sigma_B^2} = \frac{\sigma_{TOTAL}^2}{\sigma_B^2} - 1 \quad (8)$$

From the ratios of σ_{TOTAL}/σ_B given in the tables, it is seen that

$$0 \leq \frac{\sigma_{\text{MACHINE}}^2}{\sigma_B^2} \leq 5 \quad (9)$$

for the counter readings, and

$$\frac{\sigma_{\text{MACHINE}}^2}{\sigma_B^2} = 0.16 \quad (10)$$

for the d' values. As expected, machine drifts have a negligible effect upon d' values. For the signal-and-noise distribution, the average

$$\frac{\sigma_{\text{MACHINE}}^2}{\sigma_B^2}$$

is 0.3 for the nine counters, and for the noise alone distribution, it has an average value of 2 for the nine counters. On this basis, the performance of SIMRAR as a statistical measuring device is reasonably good.

Since the recording circuits of SIMRAR may be used exclusive of the simulator, some discussion of the performance of these circuits as measuring devices is desirable. Figure 66 is an experimentally-derived curve showing the resolution of the threshold in one of the amplitude discriminator circuits. This was obtained using a battery as a signal source with the 2 kc/s perturbation signal resistively coupled into the discriminator (amplifier 3 was not used). The input voltage picked off the battery was varied to obtain the points, and recording was made on a 9-millisecond sample (post interval decision time). Hence, the effect of random phasing of the perturbation signal is eliminated. The curve shows that recording may occur if the input

is within about 50 millivolts of the "true" threshold.

The drift in the recording circuits may be described by the apparent drift of the threshold levels. To obtain data on this characteristic, the recording circuits were set up with nominal differences of 100 millivolts between thresholds. (This is equivalent to about one division on the threshold Helipot dial.) A fixed dc input from a battery supply was provided, with the 2-kc perturbation signal added with a resistance network (any drift arising from amplifier 3 is therefore eliminated). Table IX tabulates the counter readings which were obtained on runs taken in one day. On each run 200 total trials were taken, requiring about half a minute of total time. The readings in Table IX are for one bank of counters, for which 100 counts maximum are possible.

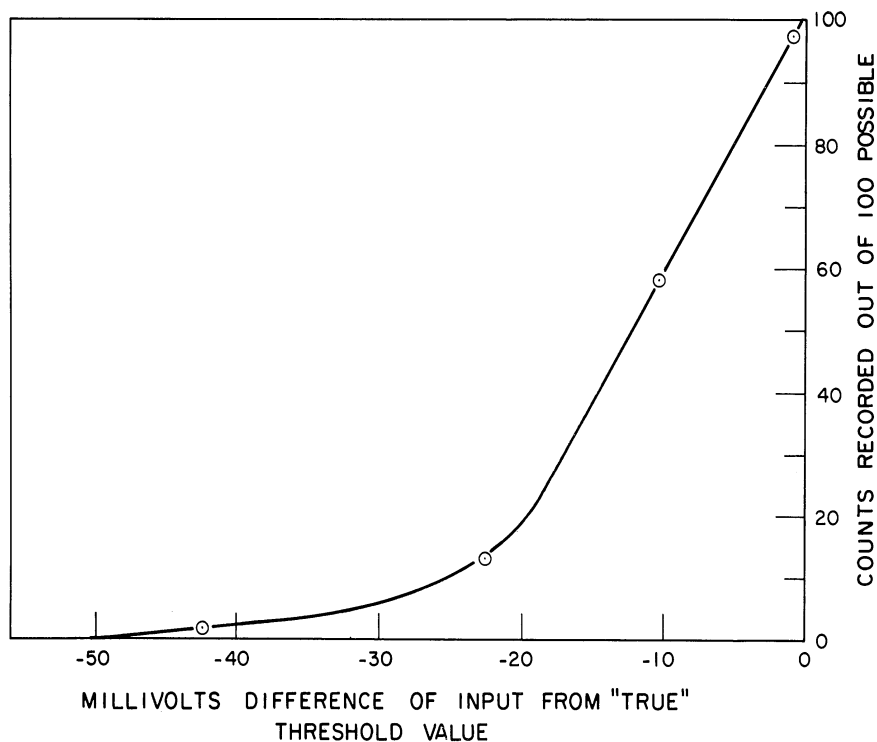


Fig. 66. Resolution of threshold level in amplitude discriminators.

TABLE IX

COUNTS RECORDED OUT OF 100 POSSIBLE

Run No.	Time of Run* (Hrs:Min)	THRESHOLD LEVEL RELATIVE TO INPUT												
		-300 mv	-200 mv	-100 mv	+100 mv	+300 mv	+400 mv	+500 mv	+600 mv	+750 mv	+500 mv			
1	0:18	100	100	100	0	0	0	0	0	0	0	0	0	0
2	3:33	100	100	100	0	0	0	0	0	0	0	0	0	0
3	3:42	100	100	100	0	0	0	0	0	0	0	0	0	0
4	5:09	100	100	100	0	0	0	0	0	0	0	0	0	0
5	5:18	100	100	100	4	0	0	0	0	0	0	0	0	0
6	5:49	100	100	100	100	0	0	0	0	0	0	0	0	0
7	5:53	100	100	100	53	0	0	0	0	0	0	0	0	0

*Each run has duration of about 30 seconds.

In runs 1 to 4, the input is straddled by thresholds which are nominally 100 mv on either side. Over a period of 5 hours, the same situation of counts recorded prevails. Considering that the threshold region (see Fig. 66) is 50 mv, it is clear that the higher threshold (+100 mv) could not have drifted down by much more than 50 mv or some recording would have occurred. Similarly, the lower threshold could not have drifted up more than 50 mv, or else less than 100 counts would have occurred on some run.

In runs 5, 6, and 7 there is nominally only 50 mv between the input level and the thresholds on either side. The drift of the upper threshold can be clearly seen, as the recorded counts go from less than 100 to the full number. Again this corresponds to a drift of approximately 50 millivolts.

Observations which have been made in other experiments with the recording circuits indicate a maximum drift of about 100 millivolts in an hour for the apparent threshold. Considering that the dynamic range of the circuits is 60 volts, this is fairly good stability. The drift expected in the simulator output would normally be considerably larger.

7. SUMMARY

The design and operation of the Simulated Receiver and Recorder equipment have been described. The equipment is used for statistical studies of signal detection by receivers employing fixed observation time, or sequential decision processes. Considerable versatility in simulation is provided through the use of operational amplifiers, a function generator, and the general switching circuits included in the equipment. The recording circuits may be used exclusive of the simulation for general statistical measurements.

REFERENCES

1. W. W. Peterson and T. G. Birdsall, "The Theory of Signal Detectability," Electronic Defense Group Technical Report No. 13, University of Michigan, June 1953.
2. W. P. Tanner, Jr. and T. G. Birdsall, "Definitions of d' and η as Psychophysical Measures," Electronic Defense Group Technical Report No. 80, University of Michigan.

DISTRIBUTION LIST

Unclassified Distribution
List - Contract DA 36-039
sc-78283

<u>Copy No.</u>		<u>Copy No.</u>	
1-2	Commanding Officer, U. S. Army Signal Research and Development Laboratory, Fort Monmouth, New Jersey, ATTN: Senior Scientist, Countermeasures Division	29	Commander, Special Weapons Center, Kirtland Air Force Base, Albuquerque, New Mexico
3	Commanding General, U. S. Army Electronic Proving Ground, Fort Huachuca, Arizona, ATTN: Director, Electronic Warfare Dept.	30	Chief, Bureau of Naval Weapons, Code RRR-E, Department of the Navy, Washington 25, D.C.
4	Chief, Research and Development Division, Office of the Chief Signal Officer, Department of the Army, Washington 25, D.C., ATTN: SIGEB	31	Chief of Naval Operations, EW Systems Branch, OP-35, Department of the Navy, Washington 25, D. C.
5	Commanding Officer, Signal Corps Electronic Research Unit, 9560th USASRU, P. O. Box 205, Mountain View, California	32	Chief, Bureau of Ships, Code 691C, Department of the Navy, Washington 25, D. C.
6	U. S. Atomic Energy Commission, 1901 Constitution Avenue, N.W., Washington 25, D. C., ATTN: Chief Librarian	33	Chief, Bureau of Ships, Code 684, Department of the Navy, Washington 25, D. C.
7	Director, Central Intelligence Agency, 2430 E Street, N. W., Washington 25, D.C., ATTN: OCD	34	Chief, Bureau of Naval Weapons, Code RAAV-33, Department of the Navy, Washington 25, D. C.
8	Signal Corps Liaison Officer, Lincoln Laboratory, Box 73, Lexington 73, Massachusetts, ATTN: Col. Clinton W. Janes	35	Commander, Naval Ordnance Test Station, Inyokern, China Lake, California, ATTN: Test Director - Code 30
9-18	Commander, Armed Services Technical Information Agency, Arlington Hall Station, Arlington 12, Virginia	36	Director, Naval Research Laboratory, Countermeasures Branch, Code 5430, Washington 25, D. C.
19	Commander, Air Research and Development Command, Andrews Air Force Base, Washington 25, D. C., ATTN: SCRC, Hq.	37	Director, Naval Research Laboratory, Washington 25, D. C., ATTN: Code 2021
20	Directorate of Research and Development, USAF, Washington 25, D. C., ATTN: Chief, Electronic Division	38	Director, Air University Library, Maxwell Air Force Base, Alabama, ATTN: CR-4987
21-22	Hqs., Aeronautical System Division, Air Force Command, Wright Patterson Air Force Base, Ohio, ATTN: WWAD	39	Commanding Officer, Director, U. S. Naval Electronic Laboratory, San Diego 52, Cal.
23	Hqs., Aeronautical System Division, Air Force Command, Wright Patterson Air Force Base, Ohio, ATTN: WCLGL-7	40	Office of the Chief of Ordnance, Department of the Army, Washington 25, D. C., ATTN: ORDTU
24	Hqs., Aeronautical System Division, Air Force Command, Wright Patterson Air Force Base, Ohio - For retransmittal to - Packard Bell Electronics, P. O. Box 337, Newbury Park, California	41	Chief, West Coast Office, U. S. Army Signal Research and Development Laboratory, Bldg. 6, 75 S. Grand Avenue, Pasadena 2, Cal.
25	Commander, Air Force Cambridge Research Center, L. G. Hanscom Field, Bedford, Massachusetts, ATTN: CROTLR-2	42	Commanding Officer, U. S. Naval Ordnance Laboratory, Silver Springs 19, Maryland
26-27	Commander, Rome Air Development Center, Griffiss Air Force Base, New York, ATTN: RCSSLD - For retransmittal to - Ohio State University Research Foundation	43-44	Chief, U. S. Army Security Agency, Arlington Hall Station, Arlington 12, Virginia, ATTN: IADEV
28	Commander, Air Proving Ground Center, ATTN: Adj/Technical Report Branch, Eglin Air Force Base, Florida	45	President, U. S. Army Defense Board, Headquarters, Fort Bliss, Texas
		46	President, U. S. Army Airborne and Electronics Board, Fort Bragg, North Carolina
		47	U. S. Army Antiaircraft Artillery and Guided Missile School, Fort Bliss, Texas
		48	Commander, USAF Security Service, San Antonio, Texas, ATTN: CLR
		49	Chief, Naval Research, Department of the Navy, Washington 25, D. C., ATTN: Code 931

<u>Copy No.</u>		<u>Copy No.</u>	
50	Commanding Officer, U. S. Army Security Agency, Operations Center, Fort Huachuca, Arizona	62-63	Commanding Officer, U. S. Army Signal Missile Support Agency, White Sands Missile Range, New Mexico, ATTN: SIGWS-EW and SIGWS-FC
51	President, U. S. Army Security Agency Board, Arlington Hall Station, Arlington 12, Virginia	64	Commanding Officer, U. S. Naval Air Development Center, Johnsville, Pennsylvania, ATTN: Naval Air Development Center Library
52	Operations Research Office, John Hopkins University, 6935 Arlington Road, Bethesda 14, Maryland, ATTN: U. S. Army Liaison Officer	65	Commanding Officer, U. S. Army Signal Research and Development Laboratory, Fort Monmouth, New Jersey, ATTN: U. S. Marine Corps Liaison Office, Code AO-4C
53	The John Hopkins University, Radiation Laboratory, 1315 St. Paul Street, Baltimore 2, Maryland, ATTN: Librarian	66	President, U. S. Army Signal Board, Fort Monmouth, New Jersey
54	Stanford Electronics Laboratories, Stanford University, Stanford, California, ATTN: Applied Electronics Laboratory Document Library	67-75	Commanding Officer, U. S. Army Signal Research and Development Laboratory, Fort Monmouth, New Jersey ATTN: 1 Copy - Director of Research 1 Copy - Technical Documents Center ADT/E 1 Copy - Chief, Countermeasures Systems Branch, Countermeasures Division 1 Copy - Chief, Detection and Location Branch, Countermeasures Div. 1 Copy - Chief, Jamming and Deception Branch, Countermeasures Div. 1 Copy - File Unit No. 2, Mail and Records, Countermeasures Div. 3 Cys - Chief, Security Division (for retransmittal to BJSM)
55	HRB Singer, Inc., Science Park, State College, Pennsylvania, ATTN: R. A. Evans, Manager, Technical Information Center	76	Director, National Security Agency, Fort George G. Meade, Maryland, ATTN: TEC
56	ITT Laboratories, 500 Washington Avenue, Nutley 10, New Jersey, ATTN: Mr. L. A. DeRosa, Div. R-15 Lab.	77	Dr. B. F. Barton, Director, Cooley Electronics Laboratory, The University of Michigan, Ann Arbor, Michigan
57	Director, USAF Project Rand, via Air Force Liaison Office, The Rand Corporation, 1700 Main Street, Santa Monica, California	78-99	Cooley Electronics Laboratory Project File, The University of Michigan, Ann Arbor, Mich.
58	Stanford Electronics Laboratories, Stanford University, Stanford, California, ATTN: Dr. R. C. Cumming	100	Project File, The University of Michigan Office of Research Administration, Ann Arbor, Michigan
59	Willow Run Laboratories, The University of Michigan, P. O. Box 2008, Ann Arbor, Michigan, ATTN: Dr. Boyd		
60	Stanford Research Institute, Menlo Park, California, ATTN: Dr. Cohn		
61	Stanford Research Institute, Menlo Park, California, ATTN: Dr. E. M. Jones		

Above distribution is effected by Countermeasures Division, Surveillance Department, USASRDL, Evans Area, Belmar, Jew Jersey. For further information contact Mr. I. O. Myers, Senior Scientist, Telephone 59-61252.

UNIVERSITY OF MICHIGAN



3 9015 02826 3682